Mercury Transport in Taconite Processing Facilities: (I) Release and Capture During Induration

Aug. 15, 2005

Michael Berndt and John Engesser
Minnesota Department of Natural Resources
Division of Lands and Minerals

Iron Ore Cooperative Research Final Report

Table of Contents

1. Abstract

With the recent emergence of atmospheric mercury as an environmental issue, taconite companies have begun looking for cost effective means to reduce mercury in stack emissions. The Minnesota Department of Natural Resources (DNR) has studied the distribution and fate of mercury at four taconite processing facilities across the Iron Range, focusing specifically on release and transport mechanisms. This document provides a mechanistic interpretation for mercury transport in induration furnaces based on data from heating experiments and from field samples collected from grates and scrubber waters at taconite plants.

During taconite processing, wet "greenballs" consisting predominantly of magnetite and possible other components (limestone flux, organic or bentonite binder, trace non-ore components) are conveyed into a furnace and heated to approximately 1200-1300ºC in the presence of air. Data from this study suggest that magnetite is first converted to a magnetite/maghemite solid-solution which attracts and collects mercury released from greenballs deeper in the furnace. Mercury release occurs when magnetite and/or magnetite/maghemite solid-solutions are heated past 450 or 500º C and converted to hematite. Wet scrubbers collect oxidized mercury from flue gases, but not volatile $Hg^0_{(g)}$. Wet scrubbers sometimes capture over 40% of the mercury released during induration, implying that extensive generation and transport of oxidized mercury can occur. On the other hand, scrubber efficiency can also be less than 10% for mercury, indicating that conditions needed for mercury oxidation are not always present. Plants having the highest capture rates for mercury, also appear to have the highest Cl and particulate fluxes, suggesting a relationship such as:

$$Hg^0_{(g)} + \underset{\text{Maghemite}}{3Fe_2O_{3(ss)}} + 2HCl_{(g)} = \underset{\text{Magnetite}}{2Fe_3O_{4(ss)}} + HgCl_{2(g)} + H_2O_{(g)}$$
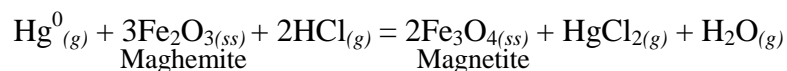
controls mercury oxidation rates during induration. Future work is planned to verify and refine flux estimates and to determine if relatively simple, passive processes such as Cl injection can increase mercury oxidation.

2. Introduction

Taconite is a very hard, relatively low grade ore that forms the basis of the iron industry in Minnesota. In 2005, six taconite companies were active, all of which mined on the Mesabi Iron Range. These include, from west to east: Keewatin Taconite Minnesota Ore Operations (Keetac), near Keewatin; Hibbing Taconite (Hibtac) near Hibbing, US Steel-Minntac (Minntac), near Mountain Iron, United Taconite (U-Tac), near Eveleth, Ispat-Inland Mining Company (IIMC; recently changed name to Mittal Steel, USA), near Virginia, and, finally, Northshore (NS) Mining, with mines located near Babbitt and ore processing facility located on the shore of Lake Superior in Silver Bay. All of these taconite plants were built decades ago to process low-grade iron ore, at a time when Hg was not an issue. Thus, atmospheric Hg emissions from taconite processing have grown with the industry, exceeding

100 kg/yr in the late 1960's, and ranging between approximately 200 and 400 kg/yr ever since (Engesser and Niles, 1997; Jiang et al., 1999; Berndt, 2003).

The Biwabik Iron Formation strikes east-northeast in a continuous band extending approximately 120 miles across northeastern Minnesota. Iron rich portions of the formation were deposited as sediments, probably as a mixture of $Fe(OH)_3$ and varying proportions of other common material (silica, carbonates, organic carbon, iron-sulfides, clays) and converted to present mineralogy during diagenesis or low-grade regional metamorphism (Morey, 1972; Perry et al., 1983; Thode and Goodwin, 1983; Bauer et al., 1985) except in the eastern sections of the formation which have been subjected to thermal metamorphism during intrusion of the Duluth Complex (Morey, 1972; Ojakangas and Matsch, 1982). By comparison, isotopic data on minerals collected from the western side of the district suggest peak "metamorphic" temperatures are less than 100 or 150º C (Morey, 1972). Because mercury volatilizes at high temperatures, this difference in metamorphic history has affected mercury distributions. Engesser and Niles (1997) and Berndt (2003) found that Hg emission factors reflected primary distribution of mercury in the concentrate, and generally increased in a westward direction across the district from 1 kg/LT (kg per million long ton) pellets at Northshore on the metamorphosed east end of the range, up to approximately 17 kg/LT on the relatively unmetamorphosed west end of the range.

During processing, magnetite is magnetically separated from other solids in the composite ore and the resulting concentrate is rolled with other minor components (fluxing agents, binders) into balls (greenballs). It is the magnetite dominated "greenballs" that are introduced into the induration furnaces where mercury emissions are generated. Because magnetite is, by far and away, the dominant mineral in concentrate and greenballs, concentrations probably represent mercury that is directly associated with magnetite, although evidence of an association with sulfur can sometimes be found, especially in the primary ore.

It is important to note that mercury emissions from taconite are generated under conditions quite distinct from those in the much better studied coal-fired power plants (see Pavlish et al, 2003, for a review). For example, the primary source of mercury emissions in coal-fired power plants is the fuel, while the primary source of mercury released during taconite processing on Minnesota's Iron Range is typically the ore (Berndt, 2003). This is partly because relatively few companies use coal to fire their pellets, while most other companies use natural gas and/or petroleum coke that contains little or no mercury. Even when coal is used, it takes only about 20 to 30 lbs of coal to fire one long ton of pellets so the amount of mercury released from the magnetite concentrate, especially on the west side of the range, greatly exceeds the amount of mercury available from the coal.

Secondly, taconite processing gases remain more oxidizing than is typical for coal-fired power plants, which consume much of the oxygen in the combustion process (Zahl et al., 1995). Oxygen is an important component for reaction with mercury molecules during transport since oxidized mercury, Hg^{2+}, is much more soluble in scrubber waters than the reduced form, Hg^0. A more oxidizing flue gas may provide more opportunities in taconite plants to control mercury using simple oxidation pathways.

Third, the released mercury is potentially exposed to large masses of heated iron oxide minerals in taconite companies that may be present, but not nearly as abundant, in power plants. This is significant, since it has been shown that iron-oxide minerals can, in some cases, promote oxidation and capture of Hg^0 (Zygarlicke, 2003; Pavlish, 2003). The more oxidizing conditions and the presence of potentially catalytic and/or reactive minerals in taconite plants can impact mercury transport and chemistry in ways not observed at coal-fired power plants.

However, one important similarity between taconite processing and coal-fired power plants is that flue gases in both types of facilities can contain chloride, an important mercury oxidation agent (Pavlish et al, 2003). In the case of power plants, the fuel is the primary Cl source, but fluxing agents and pore fluids that accompany solids into induration furnaces are the primary source of Cl in taconite processing plants.

The present study, was conducted specifically to evaluate how the presence of iron oxides and Cl in Minnesota's processing plants affect mercury transport in induration furnaces. This report represents the first of two documents being prepared on mercury transport in taconite processing facilities and details specifically mercury release and capture mechanisms that take place during induration. A second, later report will detail the ultimate fate of mercury in taconite processing plants once the mercury has been captured by wet scrubbers.

3. Methods

The present study consists of three distinct but inter-related parts:

(1) A bench-scale experimental study detailing the relationship between mercury release and mineralogy during the heating of disaggregated greenball samples from two processing plants,

(2) A field study involving systematic collection and analysis of samples of dust collected from beneath the grates in four induration furnaces, and

(3) A field study characterizing greenball and scrubber water chemistry to evaluate Hg and Cl transport and capture in four induration furnaces.

The first and second parts of this study were designed to provide fundamental information on the release temperatures and characteristics for mercury in induration furnaces. By analyzing when and where mercury is released in the furnaces, it could help to provide information on potential control options. Moreover, it was important to evaluate how the iron-oxides and volatilized mercury interact with each other. Thus, an important component of these studies was use of Mössbauer spectroscopy to evaluate oxidation of magnetite to various phases, including magnetite, magnetite/maghemite solid-solutions, maghemite, and hematite.

The third part of this study involved the collection of greenball and scrubber samples over a period of time to evaluate capture efficiency for mercury, and the factors that might affect it. Particular attention was also paid to distinguish between particulate and dissolved mercury in scrubber waters, since the relative proportion of each can affect mercury control strategies. However, that component of the study will be discussed in much greater detail in the second document in this series.

3.1. Heating Experiments

Bench-scale heating experiments were contracted with and performed by Blair Benner of the Coleraine Mineral Research Laboratory (CMRL). A full description of procedures is provided in the Appendix (section 9.3). Briefly, greenball samples collected from Hibtac (standard pellets contained about 1% limestone) and Minntac (fluxed pellets containing approximately 10% limestone flux), were dried, crushed, and then heated in either N_2 gas or air for periods of time ranging between 5 and 20 minutes. Temperatures ranged from 300 to 700ºC for Minntac samples, and from 300 to 600ºC for Hibtac samples. Mercury concentrations of run products were measured and compared to those in splits from the original sample. Iron-oxide mineralogy of selected samples was determined using Mössbauer spectroscopy at the University of Minnesota, Institute for Rock Magnetism (see section 3.4 below).

3.2. Greenball and Under-grate Dust Sampling

To further evaluate mercury transfer processes, samples were collected from beneath the grates in active induration furnaces at each of the four facilities in our study. In each case, sampling sites were chosen in consultation with mining personnel. An important distinction between plants is that two of the operations use "grate-kiln" furnaces (Minntac and United Taconite) while the other two operate "straight-grates" (Hibtac and Ispat-Inland). Grate-Kiln facilities dry and heat pellets on a grate, but final firing is done in a rotating kiln. Drying, heating, and firing procedures are all performed on the grate in a straight-grate facility, however, a "hearth layer" consisting of pre-fired pellets is added beneath fresh greenball samples to protect the grate from the intense heat used in the firing zones. Schematic diagrams for each of the induration plants are presented in the Appendix (section 9.1). This fundamental difference in plant design, when superimposed with other less distinct differences in plant operation procedures makes every plant on the Iron Range unique. Significant differences can even exist between different lines in different plants. For example, Minntac employs both ported and non-ported kilns, which affect the manner in which oxygen is added to the kiln (more exposure to oxygen takes place in a ported kiln). In our case, under-grate dust samples were collected from Line 7, which is a ported kiln. United Taconite is also a grate-kiln facility, and its kiln is non-ported.

The method of sample collection varied depending on the dust collection configuration available at the plant. For the straight-grate plants (Hibtac and Ispat-Inland), windboxes collect dust and pellet chips as the pellets move on the grate from the drying zone into the preheat and firing zones. The dust, in these cases was collected using clean aluminum pans, which were held beneath the windbox ports. The hot dust samples spilled into the pan when

the windboxes opened. Samples were covered and allowed to cool, and then sieved to remove pellet chips back at the laboratory. The <100-mesh material was analyzed for mercury at Cebam, Inc. Selected samples were also analyzed for iron-oxide mineralogy using Mössbauer spectroscopy (see section 3.4 below).

A similar process was used for collection of samples at the grate-kiln plants (Minntac and United Taconite), however, the down draft drying zone samples could not be collected dry at Minntac because the samples were only available after being mixed with process water. Solids for these samples were collected from the laundered samples on a glass fiber filter (0.7µ) and dried at 100º C overnight prior to being analyzed for mercury and iron oxide mineralogy.

In each case, information on temperature was collected (where available) for the zones where dust was sampled.

3.3. Scrubber Water and Greenball Sampling

The same four companies involved in the under-grate sample part of this project were selected for participation in our scrubber-water and greenball sampling study. Sampling sites were again chosen in consultation with mining personnel. Schematic diagrams for each of the scrubber systems are presented in the Appendix (section 9.2).

Hibtac combines scrubber water effluent from three lines into one stream flow that leads back to the concentrator. A valved sampling site was selected from this stream. Minntac Line 7 dispenses their scrubber effluent into a thickener along with other streams. Scrubber water samples were collected as a split stream of the main flow leading into the thickener. Minntac Line 4 has a valve that can be opened to collect scrubber water samples. United Taconite and Ispat Inland have recirculating scrubber systems, but continuously provide make-up water that replenishes the system and allows a continuous blow-down stream to be maintained, containing dust and dissolved components caught by the scrubber system. A valved port exists at each plant that was used for sampling of the "blow-down" water. United taconite has tandom but identical thickeners, but only one was sampled for all but the final sampling visits when both were sampled.

Berndt et al (2003) showed that scrubber waters contain a significant dissolved component in addition to mercury bound to particulates. They showed further that the ratio of particulate to dissolved mercury increases with time following collection of the sample. The dissolved mercury adsorbs to the solids. Thus, different results are obtained if a sample is filtered at the plant or if the sample is filtered later, just prior to analysis. Subsequent studies showed that the time scale for increased adsorption to particulate is on the order of minutes and hours. For the most accurate results on the relative dissolved and particulate mercury loads, it is necessary, therefore, to filter scrubber water samples within the first few minutes of sampling.

At each plant, water samples were collected in a clean two-liter plastic bottle from which sub-samples were decanted. Filtration was performed immediately using acid washed

filtration units and pre-weighed membrane filters (0.45μm, Pall Corporation). The filtered water was place in an acid washed glass jar with Teflon-lined lid. The filters containing the filtrate were placed into separate 10 ml acid washed jars and the filter weight was recorded.

All samples for mercury analyses were collected using "clean-hands, dirty-hands" procedures, whereby the clean bottles were placed into sealed plastic bags prior to leaving the laboratory and not opened except during sampling, and then again later when the analysis was being conducted. Only the designated clean-hands person, wearing clean plastic gloves, handled the sample bottles when they were outside of the plastic bag. All other sample processing was conducted quickly and efficiently by the so-called "dirty-hands" person. These procedures were implemented to minimize the risk of contamination from plant dust and of cross-contamination between samples.

In addition to these special precautions, procedures were consistently evaluated using blanks to assess the degree of mercury contamination associated with filtration and sampling. Procedural blanks were collected at each site during each visit. One bottle was filled at the sampling site with deionized water brought from the laboratory. In addition, deionized water was filtered at the sampling location and both the water and the filter were saved for analysis. The level of contamination introduced by our procedures was insignificant relative to the concentration of mercury found in samples analyzed in this study. Samples were analyzed by Cebam Analytical, Inc., located in Seattle, Washington. Filtered water samples were digested with BrCl over night, and then analyzed by $SnCl_2$ reduction, gold trap collection, and CVAFS detection (modified EPA1631). This laboratory participates in many round-robin blind sampling programs and routinely ran duplicates and standards to ensure accuracy.

Temperature, pH, and conductivity were measured on site. Temperature and pH were measured using a Beckman Model 11 meter with a Ross Model 8165BN combination pH electrode and a Beckman Model 5981150 temperature probe, while specific conductance was measured with a Myron L EP series conductivity meter.

For cation (Ca^{++}, Mg^{++}, K^+, Na^+, etc..) analyses, samples were filtered and acidified with nitric acid in the field and then analyzed by inductively coupled plasma mass spectrometry (ICP-MS) at the University of Minnesota, Department of Geology and Geophysics. For anions (Cl^-, Br^-, $SO_4^=$, etc..), samples were stored in clean plastic bottles and analyzed using ion-chromatography (IC, Dionex Ion Chromatograph fitted with a GP40 gradient pump, CD20 conductivity detector, and two AS4 anion exchange columns) at the University of Minnesota, Department of Geology and Geophysics.

Suspended Solids (scrubber dust)

Filters containing scrubber solids from the above procedures were dried at 104ºC for analysis, weighed, and digested in hot acid (HCl/HNO_3, 3/1). Particulate mercury was analyzed using $SnCl_2$ reduction and gold trap collection, followed by CVAFS detection (modified EPA1631). Certified reference materials WS-68, NIST2709, and GSR-2 were used to assess recovery and analytical accuracy. As was the case for water samples, solids were digested and analyzed by Cebam Analytical, Inc., located in Seattle, Washington.

Total suspended solids (TSS) were analyzed by filtering a two-liter sample of scrubber water collected specifically for this purpose. Solids from this sample were collected on a glass fiber filter (0.7µ), dried at 104ºC overnight, and weighed.

Greenball Samples

Greenball samples were commonly collected as a means to assess mass balance with respect to components entering and leaving the furnace (Cl and Hg, in particular).   The sample collection point, in all cases, was at the front end of the induration furnace, just prior to the point where the greenball is fed onto the grate. The samples were placed into clean, acid-washed 250 ml bottles with Teflon-lined lids. The damp greenball samples, which contain approximately 9 to 10% moisture by weight, were dried in the Hibbing laboratory and gently disaggregated prior to sending to Cebam, Inc., for total mercury analysis. Several samples were sent, as well, to the University of Minnesota, IRM, for Mössbauer spectroscopy.

To assess Cl transport and addition of other salts (Na, Ca, K, Br, SO_4) to induration furnaces, 100 grams of dry greenball material from each of the four plants was leached for approximately one week in 100 grams of deionized water. The water was then filtered and analyzed for major cations and anions using ICP-MS and ion-chromatography, respectively, at the University of Minnesota, Department of Geology and Geophysics. The resulting concentrations were reported as water-leachable salts.

3.4. Mössbauer Spectroscopy

Mössbauer spectroscopy is a sensitive technique for measuring the atomic environments of iron atoms in a compound. The technique works by measuring absorption of gamma radiation of very specific wavelengths, generated by an oscillating radioactive source material (^{57}Co). The oscillation causes a Doppler shift of the emitted gamma radiation, while a detector records absorption as a function of gamma wave frequency. Thus, results are typically presented in terms of absorption versus velocity of the radioactive source. The details of the technique are not important for this discussion, but it is important to realize that the method permits clear distinction and quantification of the relative amounts of iron that are found in the crystal lattices of magnetite and various oxidation products. Mössbauer spectroscopic measurements were made by Dr. Thelma S. Berquó at the Institute for Rock Magnetism, University of Minnesota, Minneapolis, MN. A detailed discussion of the technique and results are provided in the Appendix (Section 9.4).

Considerable importance in this study was placed on the relative distribution of iron on A and B sites of magnetite grains. As magnetite oxidizes it forms a solid solution between magnetite and maghemite. The oxygen is added by increasing the proportion of oxidized iron in A versus B sites and accommodating this change with the introduction of site vacancies in the B site.   Mössbauer spectroscopy not only evaluates mineralogy of iron oxides (e.g., magnetite, maghemite, and hematite), but determines the relative distribution of iron atoms in magnetite that are located on A or B sites. Relationship between relative absorption of gamma rays by iron on magnetite A and B sites has been related to magnetite composition by Coey (1971) and Papamarinopoulus et al. (1982), and is displayed in Figure 3.4.1.
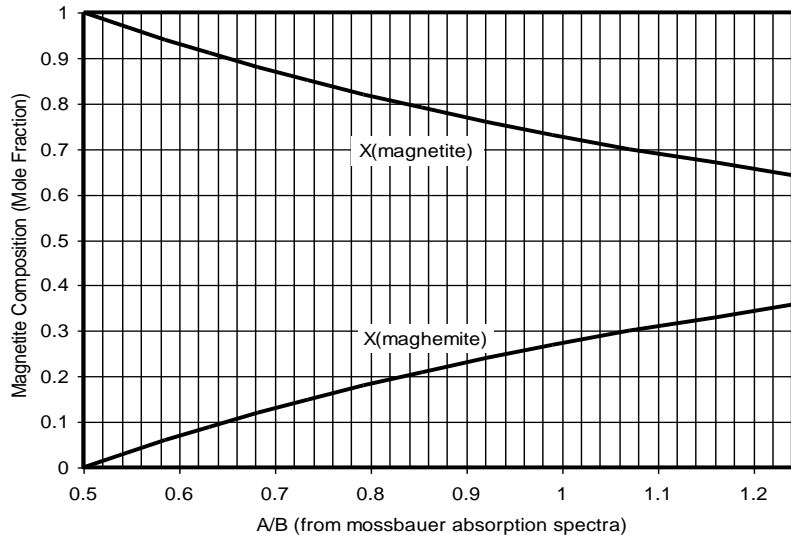
Figure 3.4.1: Ideal relationship between A/B from Mössbauer spectroscopic measurement, and magnetite/maghemite solid solution composition.

4. Results
4.1. Heating Experiments

Results from the heating experiments are provided in Tables 4.1.1 and 4.2.1, displayed in figures 4.1.1 and 4.1.2, and presented in greater detail in the Appendix (Section 9.3).

The mercury in the starting greenball sample from Hibtac was close to 21 ng/g, and the mercury remaining decreased with temperature following heating at 300 to 600ºC (Fig 4.1.1), regardless of whether heating occurred in air or in N_2 gas. However, the loss of mercury to N_2 gas was greater than the loss to air at 300 and 400ºC. The loss in mercury to N_2 and air was nearly the same, however, once the samples were heated to 500ºC. Thus, mercury is apparently less mobile in the presence of magnetite under oxidizing conditions than under a N_2 atmosphere at intermediate temperatures.

Experiments on Hibtac samples heated in air or N_2 at 450ºC for different time periods (Fig. 4.1.2) demonstrated that most of the mercury removal is rapid at this temperature, with 75% of the mercury loss occurring within the first five minutes. There was little difference in mercury loss at 450ºC for experiments conducted with N_2 or air.

Experiments conducted on Minntac greenball samples (Fig. 4.1.1) showed somewhat similar trends to those shown for Hibtac samples, however, the difference between mercury volatilization in air or N_2 was present at all temperatures, 300 to 700ºC. More mercury was released in N_2 such that volatilization was nearly complete by 600ºC. However, 27% of the mercury remained during heating of the Minntac greenball for 20 minutes at 700ºC.

Four samples from experiments on Minntac greenballs were analyzed by Mössbauer spectroscopy to gauge mineralogic changes occurring to iron oxides in the two types of

experiments (N_2 or air). The starting sample was found to contain magnetite that was slightly oxidized to begin with as indicated by A/B = 0.72 (as opposed to 0.50 for stoichiometric magnetite). Heating this material in N_2 for 20 minutes at 500ºC resulted in a decrease in the amount of magnetite and a dramatic shift in magnetite composition (to A/B = 0.59). Some of the magnetite was replaced by a mineral that appeared to be a mix of maghemite and hematite. One possibility is that the initial magnetite simply unmixed into near-stoichiometric magnetite and Fe_2O_3. It appears that much mineralogic change can occur to magnetite while heating to 500ºC for only 20 minutes, even in the absence of O_2.

Mössbauer results for samples heated in air at 400 and 500ºC revealed systematic mineralogic changes. 11% of the magnetite was replaced by hematite at 400ºC while 23% was replaced by hematite during heating at 500ºC. Moreover, the magnetite that remained became systematically more oxidized, with A/B increasing from 0.72 in the starting material, to 0.98 at 400 and 1.26 at 500ºC (approximately 27 and 36 percent maghemite component, respectively).

Table 4.1.1 Mercury concentrations for samples from heating experiments involving Greenball from Hibtac.

Temperature (ºC)	Gas	Time (min)	Hg (ng/g)
Start			20.69
			20.34
			21.39
			21.01
300 (572ºF)	Air	20	17.68
	N_2	20	9.21
400 (752ºF)	Air	20	12.72
	Air	20	11.43
	N_2	20	4.17
450 (842ºF)	Air	5	5.09
		10	3.06
		15	1.86
	N_2	5	5.87
		10	4.63
		15	2.46
500 (932ºF)	Air	20	2.61
	N_2	20	2.39
600 (1112ºF)	Air	20	1.50

Table 4.1.2 Mercury concentration and mineralogy of samples from Minntac Greenball heating experiments.

Temperature (ºC)	Gas	Time (min)	Hg (ng/g)	Mineralogy[*]	Magnetite A/B
Start			7.62	100 % mt	0.72
			7.59		
300 (572ºF)	Air	20	6.42		
	N_2	20	2.69		
400 (752ºF)	Air	20	2.89	89% mt, 11 % hm	0.98
	N_2	20	0.75		
500 (932ºF)	Air	20	3.70	77% mt, 23% hm	1.26
	N_2	20	0.92	89% mt, 11% hm?	0.59
600 (1112ºF)	Air	20	2.17		
	N_2	20	0.48		
700 (1292ºF)	Air	20	2.07		

[*] mt = magnetite solid solution, hm=hematite, hm? = sample with ambiguous pattern
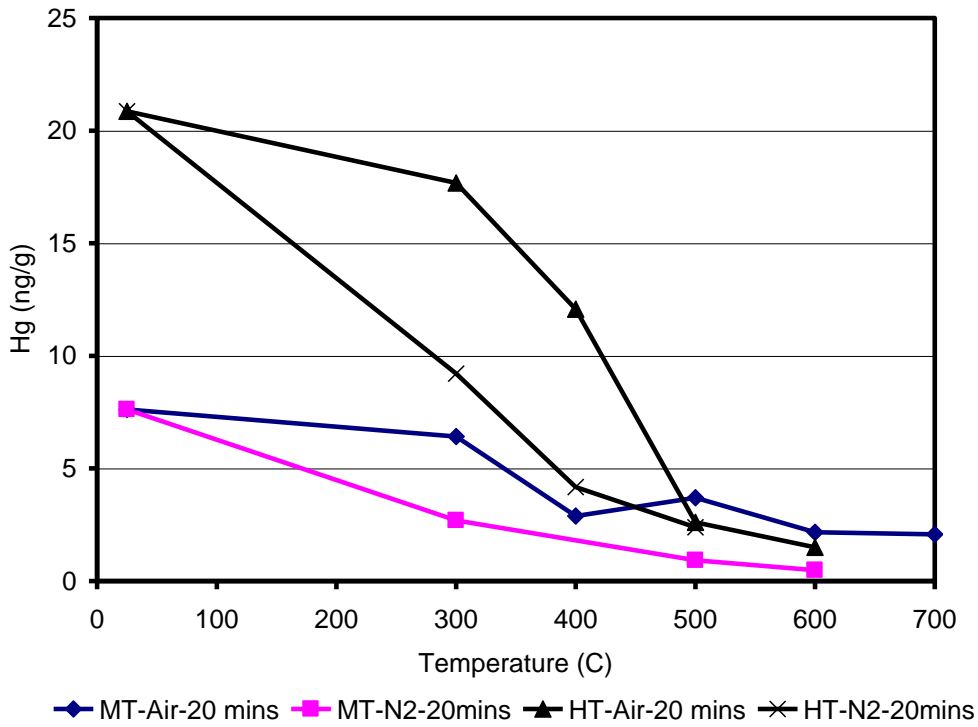
Figure 4.1.1 Mercury remaining in Minntac (MT) and Hibtac (HT) greenball samples after heating in air or nitrogen gas for 20 minutes in a tube furnace at temperatures from 300 to 700ºC.
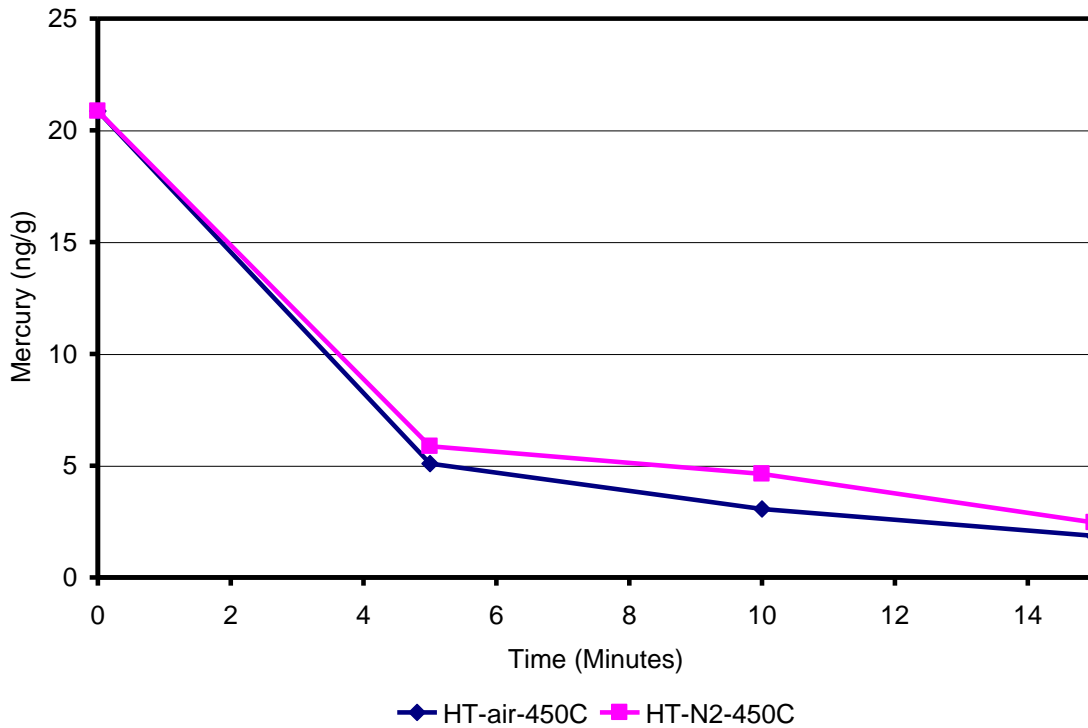
Figure 4.1.2. Concentration of mercury in samples that remained after heating Hibtac Greenball samples in air or N_2 at 450ºC for 0 to 15 minutes.

4.2. Under-grate Samples

Numerous dust samples were collected from beneath taconite grates during the course of the study and analyzed for mercury and iron oxide mineralogy (%hematite, % magnetite, % maghemite and relative A/B values (see section 3.4). Locations and dates are provided in Table 4.2.1 along with the pertinent data on location, temperatures, mercury concentration, and iron-oxide mineralogy.

Mercury concentrations were surprisingly elevated in some samples (Fig. 4.2.1). For example, concentrations of mercury reached as high as 464 ng/g in the preheat zone (Windbox 14) at Hibbing Taconite; 91 ng/g at Minntac Line 7 in the down draft drying zone (DD1), and 60 ng/g in the preheat zone at Ispat Inland (Windbox 13). These high mercury concentrations indicate that mercury released from greenball in some parts of the furnace (high temperature) can adsorb to taconite dust at lower, but still elevated, temperatures. The concentration of mercury on dust from United Taconite grates does not reach high levels, owing likely to a large dilution effect with dust that has been heated to high temperatures. Dust generation and collection at United Taconite appeared to be a much more extensive process than at the other plants.

The temperature of this adsorption process is not easy to determine due to the intense thermal gradients that exist in induration furnaces. For example, the pellet bed in taconite furnaces is only 5 to 6 inches thick in grate/kiln furnaces and about 16 inches thick in straight-grate furnaces, including a greenball layer stacked on top of a 3-inch hearth layer of pre-fired pellets. In some parts of the furnaces, depending on the plant, the temperature across the bed can differ by well over 1000ºF (or well over 500ºC) see Table 4.2.1.

Another difficulty is that although the sampling location for the dust is known, the source of the dust is not well known. Some light can be shed on this from the mineralogy of the iron oxides (Figure 4.2.2). Most of the dust in the United Taconite samples were highly elevated in hematite, suggesting much of this dust had been exposed to very high temperatures, perhaps derived from the kiln. One of the drying zone samples collected at Hibtac also had high hematite, but the source of this hematite may be the hearth layer. A dust sample collected at Minntac from the preheat zone also contained elevated hematite levels, indicating it was derived from a relatively hot zone, most likely the kiln.

Interestingly, all of the samples still contained a significant magnetite component with A/B ratios only slightly modified compared to the starting greenball samples. At Hibtac, A/B for the magnetite component increased gradually from 0.57 in the starting sample only to 0.69 for the sample in the firing zone. The change in A/B at other plants was less systematic. The A/B trend, along with decreased thermal gradients at Hibtac, and the more pronounced Hg peak suggest that the overall heating rate is low at this plant compared to others. Slower heating may lead to more time for magnetite to oxidize without converting to hematite. The oxidation of magnetite to magnetite/maghemite solid-solutions (as indicated by increasing A/B), however, is much less than that observed from the experimental run products discussed in section 4.1 where A/B increased to 0.98 after 20 minutes of heating at 400C.

Table 4.2.1 Locations, temperatures, mercury concentrations, mineralogy and magnetite composition (A/B) of samples collected from taconite plants during this study.

Plant	Location**	Overbed T (^{o}F)	Underbed T^o(F)	Hg ng/g	Mineralogy* %mt / %hm / %mh	Magnetite A/B
Hibtac	Greenball			11	96 / 0 / 4	0.57
1/27/04	UDD WB2.5	342	490	18		
	UDD WB6.5	342	490	32	50 / 50 / 0	0.61
	DDD WB8	573	340	19	94 / 6 / 0	0.62
	PH WB12	897	195	94	90 / 10 / 0	0.64
	PH WB14	1248	202	464	94 / 6 / 0	0.65
	PH WB16	1402	253	127		
	FZ WB18	2300	350	22	88 / 12 / 0	0.69
Minntac	Greenball			12	100 / 0 / 0	0.61
Line 7	DD1	654	199	91	91 / 9 / 0	0.65
7/27/04	DD2	1049	246	57		
	DD2	1443	493	66	91 / 9 / 0	0.63
	PH WB1	2076	544	15		
	PH WB3	2076	890	2.7	36 / 64 / 0	0.56
	PH WB5	2076	1215	0.7		
United	Greenball			14	100 / 0 / 0	0.59
11/29/04	DDD	525	384	24		
				24		
				21		
				24	37 / 63 / 0	0.48
	PH	1852	1291	1.7		
				1.6	35 / 65 / 0	0.59
				1.6		
				2.2		
Ispat	Greenball			10		
2/15/05	DDD WB9	720	250	7	92 / 8 / 0	0.64
	DDD WB 11	720	250	10	87 / 13 / 0	0.61
	PH WB 13	1854	250	60	91 / 9 / 0	0.60
	PH WB17	2257	700	58	92 / 8 / 0	0.61
	FZ WB 19	2332	725	26	74 / 26 / 0	0.61
	FZ WB 21	2313	730	10	63 / 37 / 0	0.75

*mt=magnetite, hm=hematite, mg=%maghemite
** UDD=Updraft drying, WB=windbox, DDD=Downdraft drying, PH=preheat, FZ=Firing Zone.
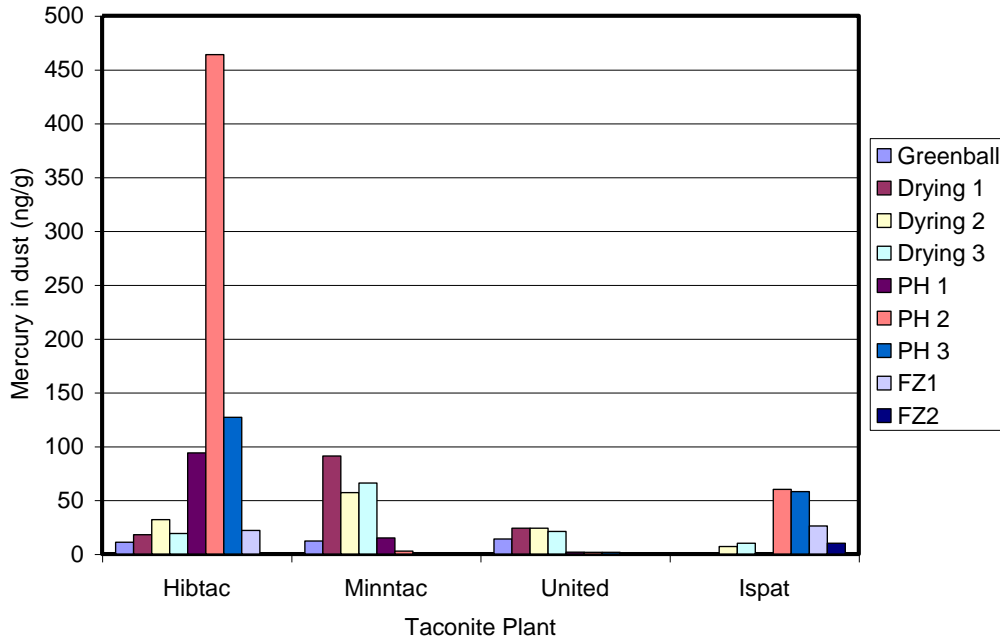
Figure 4.2.1. Mercury concentrations of dust samples collected from grates at taconite plants. Left to right on this graph for each plant represents samples collected from progressively deeper locations in the furnaces: drying zones, preheat, and firing. Hibtac and Ispat samples are from straight grates where highest mercury concentrations appear to be found in dust from preheat zones. Minntac and United, both grate-kiln plants, have their highest mercury levels in dust samples collected from the drying zones. The relative amount of mercury likely depends on the amount of dust generated, the amount of mercury available, and the specific temperatures to which the dust was exposed.
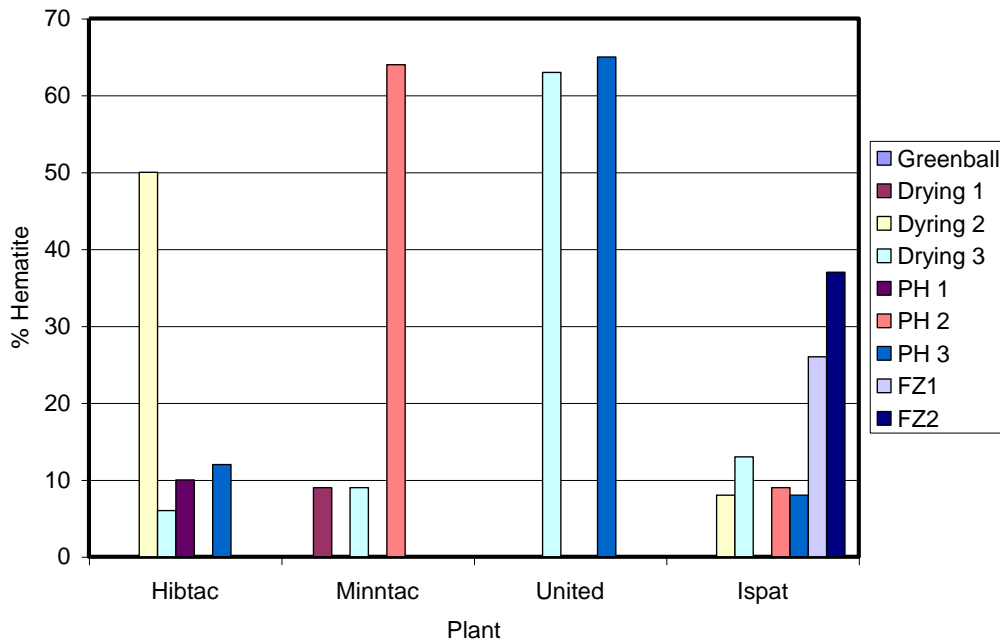
Figure 4.2.2. % Hematite for dust samples collected at taconite plants. None of the greenball samples had significant hematite and so those samples are plotted as zero % hematite on this graph. Samples from the other locations with apparent zero values were not analyzed. Temperatures representative of each zone at the time of collection are shown in Table 4.2.1.

4.3. Scrubber Water and Greenball Composition

The purpose of this portion of the study was to collect data that could be used to calculate mercury, Cl, and particulate flux values for taconite induration furnaces. By collecting information on the composition and mass of solids entering the furnace, the flux of elements and particulates can be estimated. Similarly, by collecting information on the scrubber water composition and flow rate, the flux of mercury being collected by the scrubber system can be estimated.

Greenball feed, pellet production, and scrubber water flow rates for the plants at the time of each visit are provided in Table 4.3.1. Data previous to September 2003 are included in the tables and these data were taken from Berndt *et al.* (2003). It is important to note that greenball feed rates are measured for wet samples, while most analyses are performed on a dry weight basis. Also, many of the greenball samples that are placed on a grate can break up in the furnace and are responsible for creating the dust and chips sampled in section 4.2. Another estimate of overall feed rate, subtracting moisture and loss from pellet degradation can be made using the weight of the pellet product, although in this case, oxygen is added to the Fe-oxide, increasing the weight of the overall solids, while CO_2 liberation from the limestone flux results in approximately 4-5% weight loss for the fluxed pellets produced at Minntac and Ispat-Inland.

Scrubber water flow rates are also subject to some uncertainty, depending on the plant. Hibtac and Minntac both monitor flow rates continuously and so a new reading was made during each visit. However, the flow rates at United Taconite were not measured until recently (Brad Anderson, personal communication). The value obtained (810 gpm total for two scrubbers) was used for the entire study. Plant personnel were relied on to provide flow rate estimates at Ispat-Inland which, like United Taconite, does not provide continuous measurement of flow for its scrubber. The flow rate was assumed equal to the estimated pumping rate of 350 gpm throughout the study period.

Greenball sampling began in January, 2004, and the measured mercury concentrations varied considerably: 18.6 ± 5.7 for Hibtac; 11.3 ± 3.2 for Minntac; 16.6 ± 5.1 at United Taconite; and 8.4 ± 1.3 at Ispat Inland all on a dry weight basis and in units of ng/g. At this point, sampling frequency and absence of procedural blanks was insufficient to determine if the variation was due to handling and analytical error, or if it is caused by real monthly variation in the mercury concentration of greenballs. Multiple greenball samples will be collected and sampling and drying methods will be studied further in future visits.

A similar amount of variation was observed for scrubber water samples. However, in this case, sampling frequency was greater each visit and procedural blanks were collected. At least some of the observed variation in composition is "real", although several samples with unusual values were encountered and rejected. Full data sets of data for mercury samples are provided in the Appendix (Section 9.5).

Three different mercury concentration numbers are reported in Table 4.3.2. Hg(D) is the dissolved concentration for mercury that was determined on samples that were filtered immediately upon collection in the field, and represents the best value for dissolved mercury in water as the water leaves the scrubber system. Hg(P) is the concentration of mercury in dried filtrate solids (ng/g), but only for those solids filtered from the water immediately upon sampling. Hg(T) is the total mercury in the scrubber water, and this was measured in two different ways. The first method is to add dissolved mercury to particulate mercury (as calculated from separate measurements of Total Suspended Solids, TSS, and the concentration of mercury on the suspended solids on a dry solid basis, Hg(P). The second method is to collect an unfiltered sample and send it to the laboratory for analysis of total Hg. Both methods were used here, and the average of all values for each sampling round is reported as Hg(T) in Table 4.3.2.

Other parameters of potential use for scrubber waters are reported in Table 4.3.3, including pH, indicative of capture of acidic gases, and Cl, Ca, and SO_4, elements that can change rapidly during scrubbing of process gases owing to capture of HCl and H_2SO_4. The source of Ca is unclear, but it was shown to increase significantly in scrubber waters from recirculating systems, possibly in response to reaction between solids and acid. This is demonstrated by the results of a one day test that was conducted on 2/14/05 to 2/16/05 (Table 4.3.4). In this test, scrubber water leaving the system was compared to scrubber water feed, and the change in composition was measured. HF, HCl, and H_2SO_4 (partly from oxidized SO_2) increase the most during scrubbing. Ca increases most rapidly at United Taconite which operates at pH between 3.5 and 4.5. Almost no change in Ca is observed at Hibtac and Minntac, which operated at less acidic pH values around 7.2 and 5.7, respectively.

Also reported in Table 4.3.4 are the results of greenball leach studies. The values represent leachable salts on a dry-greenball weight basis. Most of the Cl and Br in dried greenballs comes from salts that remain following evaporation of pore fluids. This concentration is used later to estimate Cl flux in furnaces.

Table 4.3.1 Plant parameters at time mercury samples were collected.

Plant	Date	Greenball Feed LT/hr	Pellet Type	Scrubber Flow (gpm)	Prod. Factor.	Pellet Production LT/hr
Hibtac	02/20/03	450	Standard	3300	0.75	338
Hibtac	05/08/03	450	Standard	3315	0.75	338
Hibtac F1-2	09/11/03	354	Standard	3000	0.75	265
Hibtac F1-3	01/27/04	397	Standard	3206	0.75	298
Hibtac F1-3	05/12/04	401	Standard	3453	0.75	301
Hibtac F1-2	07/27/04	417	1% Flux	3372	0.75	312
Hibtac F1-3	02/15/05	415	.4% Flux	3406	0.75	311
Hibtac F1-3	05/19/05	456	.4% Flux	3923	0.75	342
	Average	417		3372	0.75	313
Minntac L4	02/19/03	600	Standard	2650	0.84	504
Minntac L4	05/09/03	540	Fluxed	2645	0.84	454
Minntac L4	09/10/03	403	Standard	2980	0.84	339
Minntac L4	01/28/04	530	Standard	2900	0.84	445
	Average	518		2794	0.84	435
Minntac L7	01/28/04	530	Fluxed	2800	0.78	413
Minntac L7	05/11/04	505	Fluxed	3050	0.78	394
Minntac L7	07/27/04	605	Fluxed	2820	0.75	454
Minntac L7	12/01/04	497	Fluxed	3000	0.85	422
Minntac L7	02/16/05	490	8% Flux	3018	0.84	412
Minntac L7	05/20/05	600	8% Flux	3000	0.84	504
	Average	538		2948	0.81	433
EVTAC	02/18/03	600	Standard	810	0.87	522
United Tac	01/28/04	560	Standard	810	0.87	487
United Tac	05/11/04	604	Standard	810	0.87	525
United Tac	07/28/04	630	Standard	810	0.87	548
United Tac	11/29/04	549	Standard	810	0.87	478
United Tac	02/14/05	435	Standard	810	0.87	378
United Tac	05/19/05	598	Standard	810	0.87	520
	Average	563		810	0.87	490
Ispat Inland	02/20/03	240	Standard	350	0.62	149
Ispat Inland	05/08/03	340	Fluxed	350	0.62	211
Ispat Inland	09/11/03	510	Fluxed	350	0.62	316
Ispat Inland	01/27/04	420	Fluxed	350	0.62	260
Ispat Inland	05/12/04	501	Fluxed	350	0.62	311
Ispat Inland	11/30/04	554	Fluxed	350	0.62	343
Ispat Inland	02/15/05	428	10% Flux	350	0.62	265
Ispat Inland	05/19/05	530	10% Flux	350	0.62	329
	Average	440		350	0.62	273

Table 4.3.2 Mercury concentrations and TSS for greenball and scrubber water samples. Hg(D) = Dissolved mercury, Hg(P) = concentration of mercury in dried filtrate, Hg(T) = total mercury concentration including dissolved and particulate fractions.

Plant	Date	Greenball Hg (ng/g)	Hg(D) (ng/l)	Hg(P) (ng/g)	TSS (wt%)	Hg(T) (ng/l)
Hibtac	2/20/2003		256	1406	0.010	492
	5/8/2003		339	606	0.033	532
	9/11/2003		231	604	0.038	460
	1/27/2004	10.9	292	1484	0.018	556
	5/12/2004	16.5	237	2039	0.013	502
	7/27/2004	20.6	294	2813	0.014	688
	2/15/2005	18.6	721	2874	0.024	1410
	5/19/2005	26.4	234	8396	0.006	731
	Average	18.6	325	2528	0.019	671
	St. Dev.	5.7	164	2525	0.011	314
Minntac Line 4	2/19/2003		116	1285	0.058	1167
	5/9/2003		81	160	0.315	578
	9/10/2003		474	434	0.217	1993
	1/28/2004		164	1557	0.145	2422
	Average		209	859	0.184	1540
	St. Dev.		180	668	0.109	826
Minntac Line 7	1/28/2004		223	2489	0.041	1251
	5/11/2004	8.1	291	2723	0.052	1706
	7/27/2004	11.6	305	2564	0.095	2746
	12/1/2004	8.5	234	2830	0.075	2357
	2/16/2005	12.0	331	2855	0.058	1987
	5/20/2005	16.1	256	1360	0.100	1613
	Average	11.3	273	2470	0.070	1943
	St. Dev.	3.2	42	563	0.024	541
Evtac United	2/18/2003		64	979	0.916	6612
	1/27/2004		273	697	0.903	6571
	5/11/2004	13.2	164	594	1.270	7714
	7/28/2004	12.4	112	459	2.260	10491
	11/29/2004	13.8	32	322	2.410	7791
	2/14/2005	24.3	1440	848	2.180	19923
	5/19/2005	19.5	962	856	1.210	11829
	Average	16.6	542	616	1.866	11550
	St. Dev.	5.1	626	236	0.578	5004
Ispat	2/20/2003		1216	617	0.328	3418
	5/8/2003		852	2970	0.142	5274
	9/11/2003		1032	2094	0.175	4697
	1/27/2004		1025	1563	0.137	3166
	5/12/2004	8.9	3312	440	0.095	3730
	11/30/2004	7.2	388	1975	0.118	2719
	2/15/2005	9.9	304	4032	0.170	7157
	5/19/2005	7.5	465	2774	0.123	3865
	Average	8.4	1117	2305	0.126	4368
	St. Dev.	1.3	1465	1504	0.031	1929

Table 4.3.3 pH, Cl, Ca, and SO$_4$ concentrations for scrubber waters.

Plant	Date	pH	Cl ppm	Ca ppm	SO$_4$ ppm
Hibtac	2/20/03	6.7	86	58	325
	5/8/03	7.4	65	43	243
	9/11/03	7.5	59	44	
	1/27/04	7.3	91		335
	5/12/04	7.0		40	
	7/27/04	7.2	68	37	261
	7/27/04	7.2			
	2/15/05	7.2	98	60	368
	5/19/05	7.2	60	41	239
Minntac	2/19/03	5.6	196	138	994
Line 4	5/9/03	6.4	176	129	859
	9/10/03	6.1	162	116	
	1/28/04	4.3	194	90	870
Minntac	1/28/04	5.6	200		901
Line 7	5/11/04	5.8		106	
	7/27/04	4.0	231	115	860
	12/1/04	5.5	187	122	924
	2/16/05	5.6	208	131	964
	5/20/05	5.6	180	134	879
Evtac	2/18/03	4.2	59	180	711
United Tac	1/28/04	4.0	60	52	640
	5/11/04	3.7		106	
	7/28/04	3.5	89	140	779
	11/29/04	3.8	95	135	780
	2/14/05	4.5	82	202	780
	5/19/05	3.6	87	105	674
Ispat-Inland	2/20/03	6.7	109	45	159
	5/8/03	6.4	209	66	193
	9/11/03	7.3	160	67	
	1/27/04	6.9	195		233
	5/12/04	6.5		59	
	11/30/04	7.5	206	56	173
	2/15/05	7.2	226	54	216
	5/19/05	6.8	223	50	140

Table 4.3.4 Comparison of Greenball leach analysis and change to chemistry of scrubber water.

	F (mg/kg)	Cl (mg/kg)	Br (mg/kg)	SO_4 (mg/kg)	Na (mg/kg)	Mg (mg/kg)	K (mg/kg)	Ca (mg/kg)
Hibtac								
Greenball Leach	2.6	14.8	0.04	98	105	5.6	8.4	9.0
Scrubber Feed	13.9	92	0.41	298	85	110	18.3	61.1
Scrubber Water	22.0	98	0.43	368	85	110	18.3	59.5
Scrubber Change	8.1	6	0.02	70	0	0	0.0	-1.6
Minntac								
Greenball Leach	3.0	31.8	0.22	136	158	2.3	5.3	2.1
Scrubber Feed	3.7	180	1.30	819	105	183	27.4	128
Scrubber Water	7.0	208	1.45	964	106	182	27.6	131
Scrubber Change	3.3	28	0.15	145	1	-1	0.2	3
United Taconite								
Greenball Leach	3.2	6.8	0.05	47	69	7.6	4.4	8.6
Scrubber Feed	11.7	53	0.33	328	56	51	22.8	79
Scrubber Water	30.3	82	0.31	780	57	56	23.7	202
Scrubber Change	18.6	31	-0.02	452	1	5	0.9	123
Ispat Inland								
Greenball Leach	2.1	16.8	0.11	40	82	4.2	6.6	4.6
Scrubber Feed	5.6	109	0.87	86	68	71	8.1	31.5
Scrubber Water	28.1	226	1.95	216	83	83	11.9	53.5
Scrubber Change	22.5	117	1.08	130	15	12	3.8	22.0

5. Discussion

Results from this study have shown that mercury transport during taconite processing involves a relatively complex series of reactions, whereby some of the mercury released at high temperatures in the furnace is recaptured by magnetite and/or magnetite solid-solutions with maghemite (magnetite/maghemite solid-solutions). In all plants, however, there is also mercury captured by scrubber systems that is dissolved in solution, indicating potential importance of a molecular reaction between mercury and gaseous species, most likely Cl. To simplify the release process, we write four reactions that are shown in Table 5.1 as those most likely to impact mercury release from taconite ore. Reactions 1 and 2 represent the relative formation of magnetite/maghemite solid-solutions and hematite, while Reactions 3 and 4 represent release of mercury in reduced and oxidized form, respectively. Each of the reactions in Table 5.1 proceeds from left to right upon heating of magnetite in taconite induration furnaces, and the challenge is to determine specific processes affecting the relative rates of each process.

Magnetite oxidation to maghemite and/or magnetite/maghemite solid-solutions is important because it controls the composition of dust that may or may not react with, and ultimately help trap, reduced mercury ($Hg^0_{(g)}$) in process gases. Zygarlicke (2003) and Galbreath et al. (2005), for example, demonstrated that maghemite participates in reactions with gaseous mercury, while magnetite and hematite do not. Maghemite forms when oxygen is added to magnetite without modification of the spinel-type crystal lattice. Formation of this mineral has long been considered to take place at intermediate temperatures in induration furnaces (Papanatassiou, 1970), however, its abundance as a mineral phase, and its importance with respect to mercury transport during taconite processing, was previously unknown.

Data in the present study provide an indication of time needed for solid-solutions between magnetite and maghemite to form, but perhaps more importantly, demonstrate that mercury reacts not just with maghemite, but also with magnetite/maghemite solid-solutions that may be close in composition to magnetite. A comparison of A/B site occupancy ratios for Fe^{+3} in magnetite from experiments and grates indicate far greater formation of oxidized solid-solutions in the experiments. A/B values after 20 minutes reaction between greenball and air at temperatures of 400 and 500ºC produced magnetite having A/B = 0.98 and 1.26 (Table 4.1.2) consistent with magnetite solid-solutions composed approximately of 27 and 36% maghemite component (see Figure 3.4.1). This compares to the starting material which was composed of magnetite having A/B of 0.72, or approximately a 12% maghemite component. The magnetite in under-grate samples all had A/B between 0.48 and 0.75 (see Table 4.2.1 and compare to Figure 3.4.1) indicating that this dust had not reacted with air at elevated temperatures for sufficiently long time periods to oxidize magnetite to more maghemitic compositions. Indeed, the experiments where maghemite enriched magnetite was generated were conducted for 20 minute time intervals, while solids probably spend less than half that time reaching the firing zone in taconite induration furnaces (T = 1200 to 1300 C).

Reaction 1 in Table 5.1, therefore, does not appear to take place on a large scale, to the point where it is easily observable in dust samples from grates. We note, however, that the process may take place on a small scale during pellet induration. This is suggested by the A/B values for samples from Hibtac's grate which increased gradually from 0.57 in the starting solid to 0.69 in the firing zone. It is possible, therefore, if not likely that magnetite/maghemite solid-solutions interact with mercury, even for slight levels of maghemitization. This behavior can be understood, perhaps, by considering in more detail the steps needed for magnetite oxidation to maghemite to take place (Columbo et al., 1965; O'Reilly, 1984; Zhou et al., 2004). First, oxygen must be adsorbed to the surface of the grain. This takes place by reaction of oxygen with electrons from the Fe^{+2} component in magnetite to form Fe^{+3} and O^{-2} ions, which has the effect of extending the mineral lattice. Fe^{+3}/Fe^{+2} ratio at the mineral surface increases as a result of this interaction, and a cation site vacancy develops in the vicinity of the added oxygen. Ionic and electronic diffusion then occur to reduce the chemical gradients, and given time, the grain may become homogeneous.

Oxidation of a magnetite grain occurs from the outside in, such that full oxidation of the interior portions is diffusion limited and can only take place only as fast as Fe diffusion permits. The outer surface mineralogy and rate of mineral growth is complex, depending on temperature, humidity, oxygen availability, and nucleation effects, as well as crystal orientation (Zhou et al., 2004). Based on results from experiments and under-grate samples, conversion of magnetite to magnetite/maghemite solid-solutions can take place on relatively short time scales at 400 and 500ºC, but time scales for induration furnaces are short, so only the outer-most surfaces of magnetite grains have time to convert to magnetite/maghemite solid-solutions.

Ultimately, nearly all of the magnetite in greenballs is converted to hematite by exposure to air at temperatures of 1200 to 1300C later in the induration process. Hematite is not known as a significant oxidant for Hg^0 in flue gases at power plants (Zygarlicke, 2003). Thus, Reaction 2 in Table 1, conversion of magnetite to hematite may limit mercury oxidation and capture during induration, and the mineralogic conversion process likely signals the final release of mercury to process gases. To understand mercury transport in taconite induration furnaces, therefore, it is important to determine where magnetite and magnetite/maghemite solid-solutions convert to hematite.

For the Minntac greenball samples heated in air, it took 20 minutes of exposure at 400 and 500ºC (752 and 932ºF) to convert 11 and 23% of the solids, respectively, to hematite. Under-grate samples, obviously, require much higher reaction temperatures for this amount of hematite to form, since reaction times are much less than 20 minutes. Based on results from under-grate samples, significant hematite is observed in dust from preheat zones at both Minntac (Line 7) and United Taconite. At Hibtac and Ispat, hematite did not become a large component of the dust samples until the firing zone. In all four cases, mercury decreases become evident when hematite increases in under-grate samples, consistent with the idea that heating to the temperatures needed to generate hematite is needed to effectively release all of the mercury from magnetite/hematite solid-solutions.

This brings us to consideration of reaction 3: the conversion of mercury from its oxidized immobile form, $HgO_{(ss)}$, to its reduced and volatile form, $Hg^0_{(g)}$. The subscript "*(ss)*" in $HgO_{(ss)}$ is used to indicate Hg existing in a solid solution within magnetite/maghemite solid-solutions , however, the nature and form of this component is not well known. In primary greenball samples it likely exists initially as an element dispersed throughout the grain or, even perhaps, combined with other trace components such as sulfur. However, the high concentration of mercury observed on dust samples composed exclusively of magnetite/maghemite solid-solutions at Hibtac, leave little doubt that the element exists as a surface adsorbate on magnetite/maghemite solid-solutions in the cooler regions of the furnace where hematite has not yet begun to form. Release temperatures from experiments indicate this process is important in air at temperatures to approximately 400 or 450º (842ºF). At temperatures above this, mercury appears to have little affinity to react with magnetite solid-solutions or magnetite, perhaps signifying final conversion of the surfaces of the mineral grains to non-reactive hematite rather than to magnetite/maghemite solid-solutions.

The precise manner in which mercury evolves from the surface of magnetite/maghemite solid-solutions may provide an important constraint on the form of mercury in the resulting process gas, which can impact the behavior of mercury in wet scrubber systems. Reaction 3 in Table 5.1 is a hypothetical mechanism for producing $Hg^0_{(g)}$, the form of mercury to be avoided, if possible, because it is not captured by wet scrubbers unless subsequent chemical reactions promote oxidation in the process gas phase. One such reaction to oxidize mercury is Reaction 4, a hypothetical mechanism for generating $HgCl_2^0_{(g)}$, a molecule containing mercury in oxidized form which is easily captured by wet scrubber system and which can adsorb to solids. The relative overall rates of reactions like 3 and 4 will dictate the relative amounts of mercury released in taconite induration furnaces that can be captured either as particulate or dissolved mercury or which will be released to the atmosphere ($Hg^0_{(g)}$).

The experiments conducted for the present study (Figures 4.1.1 and 4.1.2) were conducted in the absence of HCl and, thus, provide some information on mercury systematics, although reaction times are, as discussed previously, probably too long to provide an exact analogy to processes taking place during taconite induration. For Hibtac and Minntac greenball samples over half of the mercury was released in 20 minutes of reaction at 300ºC, but only a small fraction of the mercury was driven off at this temperature during reaction in air. This suggests that at 300ºC, mercury that might have been volatilized in N_2 is instead captured and held by magnetite/maghemite solid-solutions that formed as the solid was heated. However, at 400ºC nearly half of the total mercury is released within 20 minutes, even in air. If these results were to be extrapolated to the short time scales of heating in taconite induration furnaces, it is likely that the majority of the mercury release would take place at somewhat higher temperatures than this. At 450 and especially 500º, where mercury release during N_2- and air-based experiments became similar for Hibtac samples, reactions between mercury and the surfaces of oxidation products for magnetite must no longer be as important as they were at the lower temperature. Thus, Reaction 3 in Table 5.1 appears to dominate transport at temperatures between about 300 and 400ºC, but then loses significance when temperatures approach 450ºC, perhaps commensurate with more rapid conversion of mineral surfaces from magnetite/maghemite solid-solutions to unreactive hematite.

While it is unlikely that the iron-oxide mineralogy would be strongly affected by the presence or absence of small amounts of $HCl_{(g)}$ in process gases, there is good reason to expect that the chemistry of mercury reactions taking place at the surfaces of minerals might change to favor Reaction 4 over Reaction 3 in Table 5.1. Galbreath and Zygarlicke (2000), for example, showed that the dominant transformation pathways for mercury in flue gases in coal fired power plants was by chlorination reactions at mineral surfaces on fly-ash. The reaction products were a combination of particle-bound mercury and $HgCl_{2(g)}$. Results from mercury oxidation experiments involving gas reactions with fly ash have suggested a direct role for Fe-oxides, in particular (Ghiorshi, 1999; Lee *et al.,* 2001).

The high mercury concentrations in many of the under-grate samples support this contention, as does the relatively high concentration of mercury in scrubber waters, which are present in both dissolved and particulate form. Before a role for HCl can be assessed, however, it is important to compare the relative source and abundance of HCl in taconite processing gases, as compared to flue gases from power plants. Table 5.2 presents an estimate of HCl abundance in taconite processing gases, based on feed-rate and scrubber water flow data from Table 4.3.1, greenball Cl data from Table 4.3.4, and gas flow data from Zahl et al. (1995) and personal communication (Ray Potts for Minntac, Brad Anderson for United Taconite). The predominant source of Cl is thought to be the pore fluid from processing waters and limestone flux material (Minntac and Ispat-Inland), which upon heating to 1200 to 1300ºC in the firing zone, is expected to be volatilized as $HCl^0_{(g)}$. Air containing the $HCl^0_{(g)}$ travels into the preheat and drying zones where it may react with the mercury bearing iron oxides. Since HCl is likely only released from fired pellets, the mass flux of Cl in our calculations was related to pellet production rate to account for Cl that would likely have fallen along with other material from the grates before it volatilized.

Mass balance results indicate considerable uncertainty in the amount of Cl that is volatilized from pellets, compared to the mass captured in wet scrubbers. Assuming the lower value based on flux from the firing of pellets, however, it is estimated that the taconite processing gases contain from 1 to 10 ppmv Cl. These concentrations are relatively low compared to experimental conditions where Cl generation has been shown to take place in homogenous gas phase reactions (e.g., Widmer *et al.,*1998) so it is unlikely that homogenous gas reactions with HCl will promote oxidation during taconite induration. However, Edwards et al. (2001) showed that the predominant Cl species for mercury oxidation in homogenous reactions were trace molecular species such as $Cl^0_{(g)}$ and $Cl_2^0{}_{(g)}$ which oxidize $Hg^0_{(g)}$ orders of magnitude more rapidly than HCl. It is unknown whether such metastable species exist in taconite processing gases. Another possibility is that the heterogeneous reactions between HCl and iron oxides that come into contact with the processing gas (Ghiorshi, 1999; Lee *et al.,* 2001; Zygarlicke, 2003, Galbreath et al., 2005). Certainly, there is abundant opportunity for processing gases containing $Hg^0_{(g)}$ and HCl to come into contact with iron oxides and some of the process gases obviously contain large amounts of oxidized mercury, both adsorbed to particulates and as a molecular form easily caught in wet scrubbers.

Table 5.3 was constructed as an attempt to compare estimated "capture efficiencies" for processing facilities in order to evaluate the relative effects of Cl and availability of dust particles on mercury capture. It should be noted, before comparing these values that the

estimates are highly uncertain. For example, the capture efficiency for Cl was unexpectedly poor in Table 5.2. Cl collected in the scrubber waters for three of the plants was twice as high as that calculated from greenball input values for Cl. Because no other significant source for Cl is known at these plants, it is possible that the scrubber water flow rates or the production rates may not be entirely accurate. Secondly, there is uncertainty associated with the estimate of mercury inputs into the furnace based on processes occurring in the taconite dust itself. It is unknown at this point if the mercury-bearing magnetite spilling from grates is a significant fraction of the total mercury balance, but if it is, then it would cause an underestimate of mercury capture efficiency. Finally, there was no attempt made to provide "closure" to the calculations (e.g., measuring gas chemistry) to ensure accuracy. Mercury capture efficiencies were computed in Table 5.3 for comparison purposes only. It is expected that these issues will be resolved in planned future studies.

Capture efficiencies estimated during the study (Table 5.3) varied from less than 10% to greater than 40%, with the highest recovery values being found at Minntac and United Taconite which use grate-kilns and lower values found at Hibtac and Ispat-Inland, which use straight-grates. While a simple difference in the grate type might be partially responsible for differences in capture efficiency, it is also possible that the trend is tied to differences in the concentrations of reactive components (e.g., HCl and/or iron-oxides). Combining Reactions 1, 3, and 4 in Table 5.1, for example, leads to an overall reaction describing heterogeneous oxidation of mercury by magnetite/maghemite solid-solutions and HCl, as follows:

$$Hg^0_{(g)} + 3Fe_2O_{3(ss)} + 2HCl_{(g)} = 2Fe_3O_{4(ss)} + HgCl_{2(g)} + H_2O_{(g)}.$$

$\qquad\qquad$ Maghemite $\qquad\qquad\qquad$ Magnetite

This reaction shows that if components on the left hand side of the reaction are elevated (maghemite and HCl), it will favor generation of $HgCl_{2(g)}$ relative to $Hg^0_{(g)}$ and, thus, greater capture efficiency. The company with the highest average mercury recover rate, Minntac, also has the highest Cl concentration and flux (Table 5.3). United Taconite, on the other hand, has low Cl, but has the highest Fparticulate load (also Table 5.3). These data suggest several pathways may be available to limit mercury emissions, including addition of HCl and increasing exposure of gases to maghemite or other solids.

Future studies are planned to measure gas chemistry directly in taconite induration furnaces as well as to test whether Cl injection has a direct impact on mercury oxidation and capture rates in taconite induration furnaces. Additional samples are also being collected to lessen the errors associated in estimating fluxes for Cl, Hg, and particulates. Confirmation of these trends could potentially lead to an increase in capture of mercury across the Iron Range involving manipulation of components already available in all taconite processing plants.

It should be mentioned, however, that just increasing the capture rate for mercury in induration furnaces will be insufficient to reduce mercury in taconite stack emissions. Part II of this series of papers will detail the behavior of mercury in taconite scrubber waters once the mercury is captured. Currently, three out of four plants simply recycle the captured mercury back to the induration plants. Several potential means to ensure the majority of captured mercury is routed to tailings basins, rather than back to the induration plant, are potentially

available, however, the most cost effective means to do this will likely vary at each plant, owing to differences in ore processing techniques.

Table 5.1 Primary chemical reactions that constrain mercury release, transport, and capture in taconite induration furnaces.

Number	Chemical reaction	Importance for Hg transport
(1)	$2Fe_3O_{4(ss)} + \frac{1}{2}\,O_2(g) = \ 3Fe_2O_{3(ss)}$ Magnetite $\qquad\qquad$ Maghemite	Maghemite interacts with mercury in flue gases, while magnetite does. The minerals have the same structure and form a solid solution but little is known about how mercury reacts with magnetite solid-solutions.
(2)	$2Fe_3O_4 + \frac{1}{2}\,O_2(g) = \ 3Fe_2O_3$ Magnetite $\qquad\qquad$ Hematite	Mercury is released when magnetite is converted to hematite in induration furnaces. Hematite does not interact with mercury in flue gases.
(3)	$HgO_{(ss)} = Hg^0_{(g)} + 1/2O_{2(g)}$	$Hg^0_{(g)}$ is insoluble in water and cannot be caught by wet scrubbers. $HgO_{(ss)}$ represents mercury associated with magnetite and magnetite/maghemite solid-solutions.
(4)	$HgO_{(ss)} + 2HCl_{(g)} = HgCl_{2(g)} + H_2O_{(g)}$	$HgCl_{2(g)}$ is soluble in water and the Hg^{2+} base atom can adsorb to solids. This species is more easily captured by wet scrubbers than is $Hg^0_{(g)}$.

Table 5.2 Cl-flux calculations for taconite processing facilities.

Plant	Pellet Production Rate (dry,LT/hr)	Scrubber Water flow rate (gpm)	Cl flux into furnace (g/s)	Cl flux out through scrubber (g/s)	Process Gas Flow Rate* (mscfh)	Estimated Total Cl in Gas (ppmv)
Hibtac	311	3406	1.3	1.3	20	5.2
Minntac L7	412	3018	3.7	5.3	28	10.6
United	378	810	0.7	1.4	46	1.2
Ispat Inland	265	350	1.3	2.6	18	5.8

Table 5.3 Flux calculations for taconite facilities in this study.

Plant	Particle flux to scrubber (g/sec)	Cl flux to furnace (g/sec)	Estimated Mercury Capture Efficiency
Hibtac	40	1.3	0.11 ± 0.06
Minntac 7	130	3.7	0.33 ± 0.13
United Taconite	953	0.7	0.27 ± 0.08
Isp. Inland.	25	1.3	0.14 ± 0.06

6. Conclusions

Experiments were performed and samples were collected from beneath grates and wet scrubbers in four induration furnaces to identify the primary processes affecting mercury release and capture for the taconite industry. Magnetite/maghemite solid-solutions formed during heating of the fresh magnetite-dominated greenballs in air and correspondingly, mercury release rates were greatly reduced compared to when the greenballs were heated in N_2. These results agreed with observations from under-grate samples from taconite induration furnaces which revealed considerable uptake of mercury at moderate temperatures. In general, therefore, it appears that mercury release during induration begins at approximately 450ºC and continues to unspecified higher temperatures, as the magnetite converts to hematite, which appears to exclude and not react with mercury.

Subsequent to release, mercury can resorb to magnetite/hematite solid-solutions but the overall rate of capture by wet scrubbers appears to depend both on the availability of $HCl^0_{(g)}$ and particulate phases, most likely magnetite/maghemite solid-solutions, consistent with a reaction such as:

$$Hg^0_{(g)} + Fe_2O_{3(ss)} + 2HCl_{(g)} = 2Fe_3O_{4(ss)} + HgCl_{2(g)} + H_2O_{(g)}$$
$$\text{Maghemite} \qquad\qquad \text{Magnetite}$$
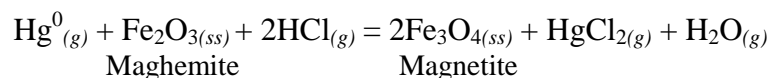
Despite the considerable uncertainty that exists in computation of mass fluxes for mercury, chloride, and particulates in taconite induration furnaces, the relationships observed in this study provide evidence that relatively simple procedures involving injection of Cl and/or maghemite/magnetite may provide a relatively cheap and simple means to control mercury emissions during induration at taconite processing facilities.

7. References

Bauer, M. E., Hayes, J. M., Studley, S. A., and Walter, M. R. (1985) Millimeter-scale variations of stable isotope abundances in carbonates from banded iron-formations in the Hammersly Group of Western Australia. Econ. Geol. 80, 270-282.

Berndt, M. E. (2003) *Mercury and mining in Minnesota*. Final report, Minnesota Department of Natural Resources, 58p.

Berndt, M. E. and Engesser, J. (2003) On the distribution of mercury in taconite plant scrubber systems. Minnesota DNR report prepared for MPCA. 30 p.

Colombo, U., Gazzarrini, F., Lanzavecchia, G., Sironi, G. (1965) Magnetite oxidation: a proposed mechanism. *Science*, 147, 1033.

Coey, J.M.D., Morrish, A. H., Sawatsky, A. Mössbauer study of conduction in magnetite. J. Phys. (1971) C1-32, 271-273.

Edwards, J. R., Srivatava, R. K., and Kilgroe, J. D. (2001) A study of gas-phase mercury speciation using detailed chemical kinetics. J. Air. Waste. Man. Assoc., 51, 869-877.

Engesser, J. and Niles, H. (1997) Mercury emissions from taconite pellet production. Coleraine Minerals Research Laboratory, Report to MPCA: U of M contract # 1663-187-6253. 16 pages plus tables, figures and appendices.

Galbreath, K. C. and Zygarlicke, C. J. (2000) Mercury transformation in coal combustion flue gas. Fuel Processing Tech. 65, 289-310.

Galbreath, K. C., Zygarlicke, C. J., Tibbetts, J. E., Schulz, R. L., and Dunham, G. E. (2005) Effects of NO_x, α-Fe_2O_3, δ-Fe_2O_3, and HCl on mercury transformations in a 7-kW coal combustion system. Fuel Processing Technology, 86, 429-488.

Ghiorshi, B. S. (1999) Study of the fundamentals of mercury speciation in coal-fired boilers under simulated post-combustion conditions. EPA-600/R-99-026, United States EPA Office of Res. and Development, NC.

Jiang, H., Arkly, S., and Wickman, T (2000) Mercury emissions from taconite concentrate pellets- stack testing results from facilities in Minnesota. Presented at USEPA conference "Assessing and managing mercury from historic and current mining activities". San Francisco, November 28-30, 18 pages.

Lee, L. W., Srivistava, R. K., Kilgroe, J. D., and Giorshi, S. B. (2001), Effect of iron content in coal combustion fly ashes on speciation of mercury. Proc. 94th., A&WMA Annual Meeting, Air and Waste Management Association, Pittsburgh, PA.

Morey, G. B. (1972) Mesabi Range. In: Geology of Minnesota: A centennial volume. P.K. Sims and G. B. Morey (eds), Minnesota Geological Survey, St. Paul, MN. 204-217.

Ojakangas, R. W. and Matsch, C. L. (1982) Minnesota's Geology. University of Minnesota Press, Minneapolis. 255 p. O'Reilly, W. (1984) Rocks and Rock Magnetism, Chapman and Hall, NY.

Papamarinopoulus, S., Readman, P. W., Maniatis, Y., and Simopoulos, A., 1982, Magnetic Characterization and Mössbauer spectroscopy of magnetic concentrates from Greek lake sediments. Earth Plant Sci. Letters, 57, 173-181.

Papanatassiou, D. J. (1970) Mechanisms and Kinetics Underlying the Oxidation of Magnetite in the Induration of Iron Ore Pellets. University of Minnesota, Duluth, Unpublished PHD Thesis. 134 p.

Pavlisch, J. H., Sondreal, E. A., Mann, M. D., Olson, E. S., Galbreath, K. C., Laudal, D. L., and Benson, S. A. (2003), Status Review of Mercury. Control Options for Coal-fired Power Plants. Fuel Processing Technology 82. 89-165.

Perry, E. C., Jr., Tan, F. C., and Morey, G. B. (1973) Geology and stable isotope geochemistry of the Biwabik iron-formations. Econ. Geol. 68, 1110-1125.

Thode, H. G. and Goodwin, A. M. (1983) Further sulfur and carbon isotope studies of late Archaen Iron-Formations of the Canadian Shield and the rise of sulfate reducing bacteria. Precambrian Research, 20, 337-356.

Widmer, N. C., Cole, J. A., Seeker, W. R., and Gaspar, J. A. (1998) Combust. Sci. Tchnol. 134, 315-326.

Zahl, R., Haas, L, and Engesser, J. (1995) Formation of NO_X in Iron Oxide Pelletizing Furnaces. Iron Ore Cooperative Research (MnDNR), 43 p. plus tables and figures.

Zhou, Y., Xuesong, J., Mukovskii, Y, and Shvets, I. (2004) Kinetics of oxidation of low-index surfaces of magnetite. J. Phys: Condensed Matter. 16, 1-12.

Zygarlicke, et al. (2003) Experimental Investigations of Mercury Transformations in Pilot-Scale Combustion Systems and a Bench-Scale Entrained-Flow Reactor. University of North Dakota Energy and Environmental Research Center Technical Report. 22 p.

8. Acknowledgments

9. Appendices
9.1. Taconite Induration Furnaces
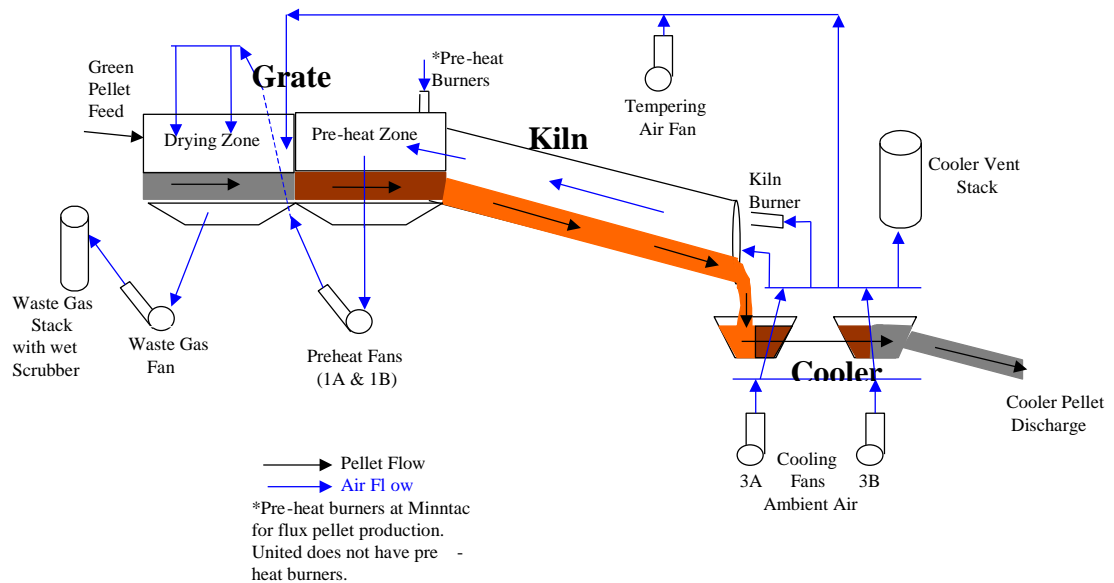
Figure 1. Diagram of a grate-kiln taconite pellet induration process (used at Minntac and United Taconite). Fresh, wet pellets (termed green balls) fed into the system (on the left side) are systematically dried, heated, and hardened into pellets as they pass from the drying zone to the rotating kiln. Drying and heating is accomplished using gases, that are generated by cooling of the hot pellets and burning of fresh fuels in the kiln. The gases interact with pellets in the kiln, and are passed through pellet beds in the drying and pre-heat zones. The gases carry mercury and dust to the wet scrubber systems that were sampled in our study. The preheat burner near the center of the diagram is used only for fluxed pellet production.
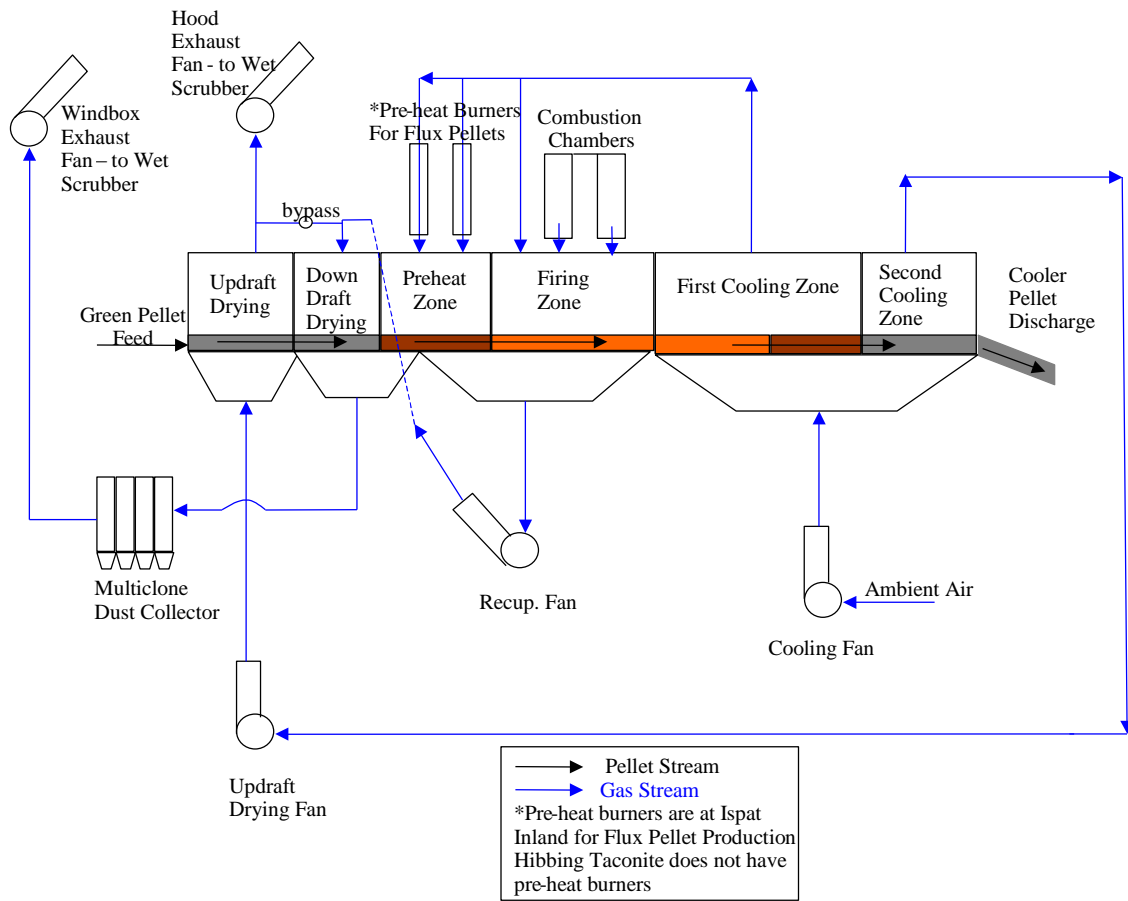
Figure 2. Diagram of a straight-grate taconite pellet induration process (used at Hibtac and Ispat Inland). Fresh pellets are carried on a grate through a furnace and cooled by fresh air passed through the pellet bed. The air used for cooling the hot pellets and gases generated in the firing zone are used for drying and heating the pellets.

9.2. Taconite Scrubber Systems

Hibbing Taconite Company Scrubber Flow Diagram
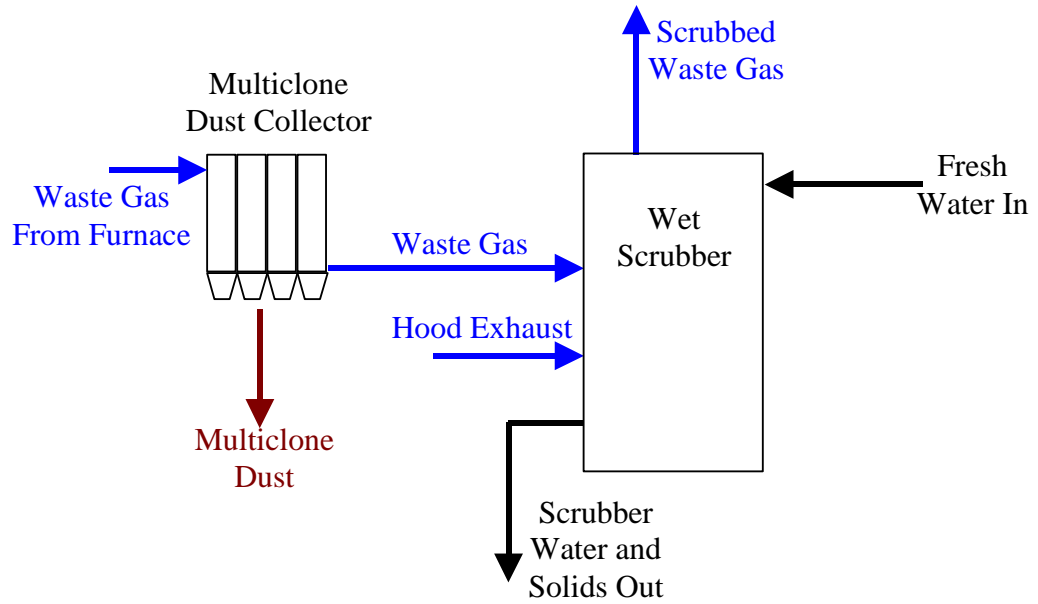
Minntac Scrubber Flow Diagram
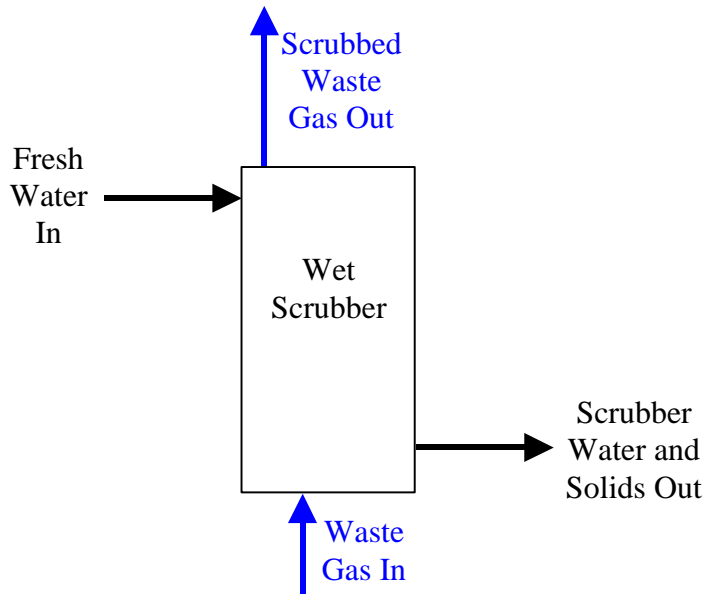
United Taconite Scrubber Flow Diagram

Scrubbed
Waste Gas

Fresh Slat
Water In

Wet
Scrubber

De-mister
Tank

Waste Gas
from Furnace

Thickener

Sump

Solids and Water
Underflow
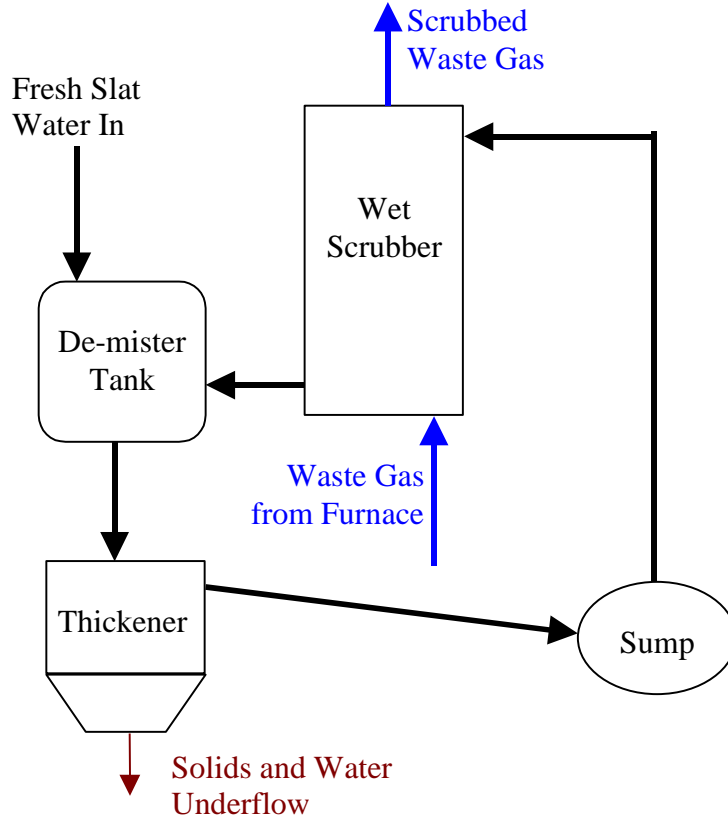
Ispat-Inland Scrubber Flow Diagram

Scrubbed
Waste Gas

Recycled
Scrubber
Water In

Wet
Scrubber

Multiclone
Dust Collector

Scrubber
Sump

Waste Gas

Waste Gas
From Furnace

Hood Exhaust

Scrubber
Water and
Solids Out

Multiclone
Dust
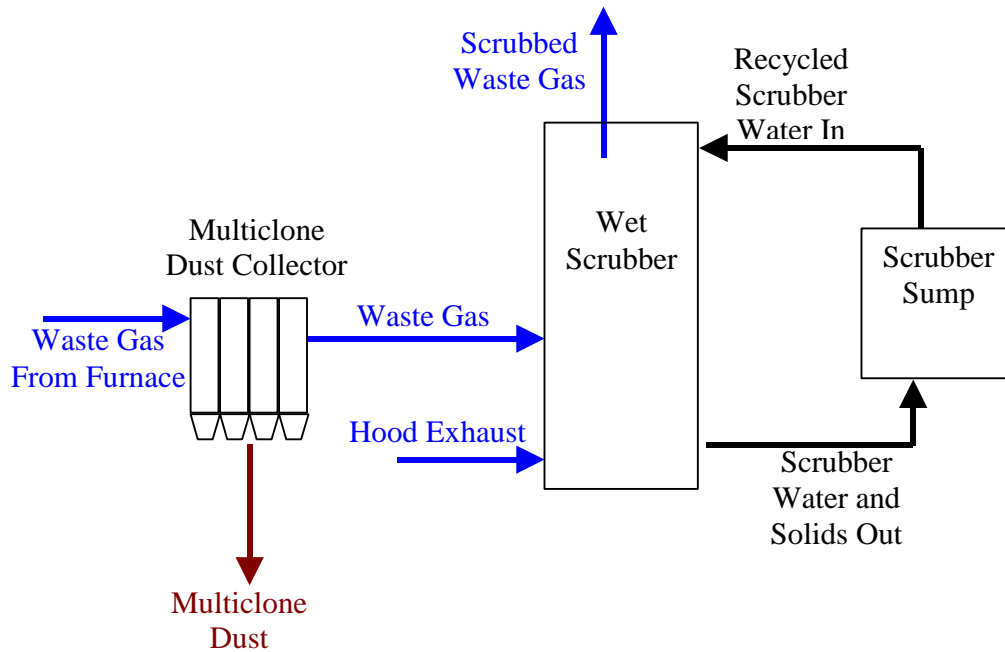
9.3. *Heating Experiments (B. Benner, CRML)*

(Scanned text from hard copy original)

Mercury Release from Taconite During Heating

Blair Benner (CMRL report TR-05-06/NRRI/TR-2005-17) June 15, 2005

Introduction:

The taconite industry is under pressure to reduce the emissions of mercury from their induration process. Previous studies have indicated that greater than 90 percent of the mercury in the green balls being fed to the induration process is vaporized during the induration. The Minnesota DNR is in the process of conducting a bench-scale study to determine the rate of mercury release as a function of temperature during the heating of taconite. This program is a supplement to that work. The objectives of this program were to determine the role of oxidation in the release of mercury at various temperatures and to provide samples of heated material for Mossbauer spectroscopic analysis.

Test Procedure and Results:

In consultation with the DNR, samples of green balls were obtained from Minntac (Line 6) and Hibtac. The green balls were dried at 100 C, crushed, and blended to provide two feedstocks for the testing. Head samples were taken for mercury and Mossbauer analyses. An electrically heated tube furnace with a built-in temperature controller was used for all of the tests. A 7/8-inch ID combustion tube was placed inside the tube furnace. Temperature measurements were taken inside the combustion tube at the center and 3/4 and 1.5 inches from each side of the center. The temperatures in the 3 inch zone ranged from 500 to 505 C.

The test procedure was as follows: The furnace was heated to the desired temperature. If the test was to be conducted in a nitrogen atmosphere, the combustion tube was purged for 20 minutes with nitrogen being added at the rate of 0.67 l/min. An empty 3-inch long combustion boat was weighed. The boat was filled with the desired sample of dried green balls and re-weighed. The loaded boat was placed in the center of the heating zone and either air or nitrogen was added to the tube at the rate of 0.67 l/min. After 20 minutes, the boat was removed from the hot zone. In the case of tests in nitrogen, the boat was kept in the cool end of the combustion tube for 10 minutes under nitrogen to prevent oxidation. In the case of tests in air the boat was removed from the combustion tube to cool. A portion of the cooled sample was submitted for mercury analyses and a portion was sent out for Mossbauer analysis. With each set of mercury analyses, a taconite concentrate standard1 containing 14 +/- 1.2 *nglg* Hg was also run. The results for the Minntac Line 6 green balls are given in Table I. At all temperatures there was a greater release of mercury in nitrogen than in air. With the exception of the test run at 5OO C, there is a steady increase in the amount of mercury released with increasing temperature. The fact that the 500 C tests were the first tests run may have contributed to the slight anomaly. It is apparent that heating in air retards the release of mercury. Even heating to 700 C in air

resulted in more than twice the concentration of mercury remaining in the solids compared with heating to 400 C in nitrogen *(2.07 ng/g* vs. 0.75 *ng/g).*

The results for the tests with Hibtac green balls are given on Table II. The results were similar to the ones from the Minntac green balls at lower temperatures. Namely, that more mercury was released in nitrogen than in air. The main difference between the two green balls was seen above 400°C. Above 400°C with the Hibtac green balls there was essentially no difference between air and nitrogen, while with the Minntac green balls there was always a significant difference between air and nitrogen.

To investigate the effect time may have on the mercury release, Hibtac green balls were tested at 450°C. The samples were placed in the furnace for 5, 10 and 15 minutes in air and in nitrogen. The times *refer* to the time from insertion of the boat until removal. In these tests all of the boats including those from the nitrogen tests were removed from the tube to cool. The test results, Table II, indicate that a significant amount of the mercury was released in 5 minutes with the release increasing with time.

Conclusion:

This test work has shown that the release of mercury during induration is related to temperature, time and atmosphere. Since Minntac green balls contain flux and caustic soda, the differences in chemistry may have had an effect on the mercury release. The rapid release of mercury with the Hibtac green balls suggests that in plant practice the mercury is released early in the process. Although time tests were not run on the Minntac green balls, it is probable that the release from Minntac green balls would also be rapid. This would suggest that the mercury is released on the grate in plant practice and, therefore, there should be little difference between straight-grate and grate-kiln plants. Since atmosphere appears to have an effect on mercury release, tests should be run in an atmosphere similar to that found in the plant machines.

Reference:

1. B. R. Benner, "Preparation of Mercury Standard from Taconite," CMRL technical report TR-01-16, September 25,2001.

Table 1- Summary of Tests with Minntac Green Balls Air and Nitrogen Flow Rates = 0.67 l/min

Sample	HQ, ng/g	Sample Wt., g	ng Hg removed
Minntac Line 6 Green Balls	7.62		
Minntac Line 6 Green Balls	7.59		
AVG	7.61		
300°C in Air	6.42	4.6588	5.55
300°C in Nitrogen	2.69	4.7760	23.51
400°C in Air	2.89	4.0025	18.89
400°C in Nitrogen	0.75	4.1379	28.36
Standard (14 +/-1.2 ng/g)	14.20		
500°C in Air	3.70	3.8806	15.17
500°C in Nitrogen	0.92	3.9669	26.53
600°C in Air	2.17	4.7994	26.12
600°C in Nitrogen	0.48	4.7716	34.02
700°C in Air	2.07	5.0308	27.84
Standard (14 +/-1.2 ng/g)	13.57		

Table II - Summary of Tests with Hibtac Green Balls Air and Nitrogen Flow Rates = 0.067 l/min

Sample	HQ, ng/g	Sample Wt, g	ng Hg removed
HTC Green Balls, Head	20.69		
	20.34		
	21.39		
	21.01		
AVG, Head	20.86		
300°C in air	17.68	5.3661	17.05
300°C in nitrogen	9.21	5.2255	60.86
400°C in air	12.72	5.3464	43.50
400°C in air (repeat)	11 .43	5.3845	50.77
400°C in nitrogen	4.17	5.3847	89.86
500°C in air	2.61	5.4278	99.02
500°C in nitrogen	2.39	5.5266	102.04
600°C in air	1.50	5.1340	99.40
Standard (14 +/-1.2 ng/g)	13.57		
Standard (14 +/-1.2 ng/g)	14.96		
450°C in air for 5 min	5.09	5.2466	82.69
450°C in air for 10 min	3.06	5.5479	98.71
450°C in air for 15 min	1.86	5.4438	103.39
450°C in N2 for 5 min	5.87	5.2495	78.69
450°C in N2 for 10 min	4.63	5.4550	88.52
450°C in N2 for 15 min	2.46	5.3369	98.19
Standard (14 +/-1.2 ng/g)	15.12		

9.4. *Mössbauer Report (T. Berquo, IRM)*

Mössbauer spectroscopy analyses of taconite dust samples

Thelma S. Berquó, Institute for Rock magnetism, Department of Geology and Geophysics, University of Minnesota, Minneapolis, MN 55455

1. Introduction

Mössbauer spectroscopy is used routinely as an analytical tool in many different areas of science, for example physics, biology and geology. In geology, materials like soils, sediments and rocks are frequently studied. Murad and Cashion (2004) introduced some useful information related to Mössbauer spectroscopy and mineral processing. This is a powerful technique to study iron ores, since the Fe is extremely abundant and mineral transformations are common during the processing of iron-containing ores. By using Mössbauer spectroscopy it is possible to observe the presence of different iron phases (magnetite, maghemite and hematite) or a mixture of these iron oxides during the processing.

Magnetite is a stable mineral found in iron deposits of northern Minnesota. This mineral oxidizes to Fe^{3+}-oxides like maghemite or hematite. The specific mechanism of oxidation is complex and some information can be found at the literature, p. ex., Colombo et al. (1965), O'Reilly (1984) and Zhou et al. (2004).

The iron ore in northern Minnesota contains trace mercury which may be released during mineral processing. This mercury could be released during transformation of magnetite to another phase. The goal of this project is to determine and quantify relationships between iron oxide transformation and mercury release during mineral processing.

Mössbauer spectroscopy is a nuclear techinique and has a rich literature where many books (Greenwood and Gibb, 1971, Cornell and Schwertmann, 1996, Murad and Cashion, 2004, among other) discuss the methods in details. Below we present a short introduction to Mössbauer spectroscopy adapted from Dickson and Berry (1983), some information about the hyperfine parameters obtained by the technique and finally the experimental data obtained during this study on taconite processing samples.

2. Mössbauer spectroscopy

The energy of a nucleus situated in an atom and in a solid is modified very slightly by the environment of the nucleus. Mössbauer spectroscopy is a technique which enables these energy levels to be investigated by measuring the energy dependence of the resonant absorption of Mössbauer gamma rays by nuclei. Hence, the hyperfine interaction between the nucleus and its surrounding electrons are investigated by this technique using the nucleus itself to probe its chemical environment.

The most usual experimental arrangement for Mössbauer spectroscopy, and the one used in this study, involves a radioactive source containing the Mössbauer isotope source material in an excited state and material to be investigated containing this same isotope in its ground state. The source used in this work was the normally radioactive ^{57}Co which undergoes a spontaneous electron capture transition to give a metastable state of ^{57}Fe which in turn decays to the ground state via a gamma ray cascade which includes 14.4 keV gamma rays useful for Mössbauer studies of material containing iron atoms. Gamma rays emitted by the source are partially absorbed by the iron atoms before passing through a suitable detector.

A critical aspect of Mössbauer spectroscopy is the systematic varying of gamma ray energy through movement of the source and its resulting Doppler shift. Resonant absorption occurs when the energy of the gamma ray exactly matches the nuclear transition energy for iron nuclei in the absorber and the Doppler shifting of the energy provides the means to precisely match those energies at very specific source velocities. Thus, the resulting Mössbauer spectrum consists of a plot of gamma ray counts against the velocity of the source. The spectrum is accumulated for a period typically of the order of hours or days and is a function of the concentration of Fe atoms in various chemical states within the absorbing material. Relative concentration of different chemical forms for iron atoms in a solid source provides quantitative information on the mineralogy of the samples. Further information, useful for mineralogic identification and provided by the spectrums, include hyperfine parameters: isomer shift (IS), quadrupole splitting (QS) and magnetic hyperfine field (B_{hf}).

The **isomer shift** of the Mössbauer spectrum is a result of the electric monopole interaction between the nuclear charge distribution over the finite nuclear volume and the electronic charge density over this volume. The **quadrupole splitting** obtained from the Mössbauer measurement involves both nuclear quantity, the quadrupole moment, and an electronic quantity, the electric field gradient. This parameter reflects the symmetry of the bonding environment and the local structure in the vicinity of the Mössbauer atom. Finally, the **magnetic hyperfine field** is the interaction between the nuclear magnetic moment and the net effective magnetic field that is felt by the nucleus.

3. The Iron Oxides

Iron occurs in minerals both as a major constituent and also as an impurity. Magnetite, maghemite, and hematite, the three primary minerals of interest here, were characterized with Mössbauer spectroscopy. Detailed Mössbauer information for these minerals, briefly reviewed below, can be found in the following sources: Long and Grandjean, 1993; Vandenberghe et al., 1990; Cornell and Schwertmann, 1996; Vandenberghe et al., 2000; Murad and Cashion, 2004.

Magnetite is a ferrimagnetic mineral and differ from the other iron oxides because contain both divalent an trivalent iron, with structural formula $(Fe^{3+})_A[Fe^{2.5+}]_BO_4$ in which the B site, with ferrous and ferric ions, merge into $Fe^{2.5+}$ due to a fast electron hopping above the Verwey transition (~120 K). Mössbauer spectrum at room temperature

can be fitted with two well-known distinct sextets with typical hyperfine parameter for the sextet corresponding to high spin Fe^{3+} on the tetrahedral site (B_{hf}=49.2 T; QS=0.02 mm/s; IS= 0.26 mm/s) and the other one to $Fe^{2.5+}$ on the octahedral site (B_{hf}=46.1 T; QS=-0.02 mm/s; IS= 0.67 mm/s).

Magnetite forms a complete solid solution series with **maghemite**, a mineral similar to magnetite in structure, but where all or most Fe is in the trivalent state and cation vacancies, which are necessary to compensate for the oxidation of Fe^{2+}, are all located on the B-site; resulting in the formula $(Fe^{3+})_A[\square_{1/3}Fe^{3+}_{5/3}]_BO_4$ ($\square$ represents vacancies). The room temperature Mössbauer spectrum of maghemite consists of a slightly asymmetric sextet with hyperfine parameter B_{hf}=50.0 T, QS~0 mm/s and IS=0.35 mm/s.

For ideal magnetite the sextet area ratio A/B is 1:2 or 0.5. However, deviations from the ideal ratio are often observed due to oxidizing effects as magnetite becomes more maghemite-like. In such cases, there is a decrease in the $Fe^{2.5+}$ component and increase in Fe^{3+} component on the B-site. The B-site Fe^{3+} hyperfine parameters are similar from those of the A-site and together with introduction of vacancies this will result in a decrease of the B-site sextet area and an apparent increase of that of the A-site. Thus, the area ratio A/B can be used to determine the degree of oxidation of the magnetite, prior to formation of end-member maghemite or other phases.

Hematite is the most stable iron oxide phase in air and it is represented by the formula Fe_2O_3. The material has red color and it is an important constituent in iron ores. At room temperature the Mössbauer spectrum of a stoichiometric hematite consists of a sextet with the following hyperfine parameters B_{hf}=51.8 T, QS=-0.20 mm/s and IS=0.37 mm/s. Hematite has the same chemical composition as maghemite, but it is a distinct mineral with different, generally less reactive, chemical behavior.

4. Taconite study

Taconite production involves the fine grinding and magnetic separation of magnetite from the iron ore and the conversion of the magnetic concentrate into pellets. The magnetic concentrate is composed mostly of magnetite which is rolled with other minor components (fluxing agents, binders, water) into balls (greenballs). The magnetite (or greenballs) is introduced into the indurating furnaces where mercury emissions are generated upon heating to high temperatures (Berndt, 2003).

The samples studied here are from four taconite processing facilities: Hibtac, Minntac, United Taconite and Ispat Inland. All Mössbauer spectra were measured at room temperature. A conventional constant-acceleration spectrometer was used in transmission geometry with a ^{57}Co/Rh source, using a α- Fe at room temperature to calibrate isomer shifts and velocity scale.

The hyperfine parameters obtained after fitting are presented from Table 1 to 6, as well as the fitted spectra are showed from Figure 1 to 6. Magnetite was noticed in all samples but with slightly changing ratio A/B, which is related to oxidation degree, with the increase

of the heating temperature. The main feature observed in these samples were variations in hematite amount and sometimes magnetite becoming well crystallized (ratio A/B~0.5) upon heating. Thermal treatment is a useful and very common method to provide well crystallized synthetic samples, where crystal defects like vacancies can be eliminated. The hematite is resultant from transformation of magnetite into hematite, the transformation of magnetite grains bigger than 300 nm in air atmosphere will produce hematite, even at low temperatures, and maghemite formation is by-passed (Cornell and Schwertmann, 1996). Maghemite was observed in the starting material from HIBTAC plant, but upon heating only oxidized magnetite (A/B > 0.5) and hematite were observed.

Several greenball samples that had been heated to temperatures up to 500° C in either air or N_2 gas for 20 minutes each at another laboratory were analyzed for mineralogy. These data are presented in Table 6 and Figure 6. With increase of the temperature it is possible to observe the increase of hematite amount, for samples heated in air. There is also a temperature dependent increase in A/B for the residual magnetite that does not convert to hematite. This magnetite is being progressively oxidized to magnetite/maghemite solid-solutions. For the sample heated at 500 ^{o}C at N_2 atmosphere we could identify the presence of 89% of magnetite which was became more stoichiometric (A/B=0.59) and 11% of another phase which could be represented by a combination of maghemite and hematite. The starting mineral appears to have unmixed. Therefore, a mineralogic change was observed in both cases, but each atmosphere produced different final products.

5. References

Berndt, M. E. (2003) *Mercury and mining in Minnesota*. Final report, Minnesota Department of Natural Resources, 58p.

Colombo, U., Gazzarrini, F., Lanzavecchia, G., Sironi, G. (1965) Magnetite oxidation: a proposed mechanism. *Science*, 147, 1033.

Cornell, R. M. and Schwertmann, U. (1996) *The iron Oxides: structure, properties, reactions, occurrence and uses*. VCH, Weinheim, 573p.

Dickson, D. P. E. and Berry, F. J. (1986) *Mössbauer spectroscopy*. Cambridge University Press, Cambridge, 274p.

Greenwood, N. N. and Gibb, T. C. (1971) *Mössbauer spectroscopy*. Chapman and Hall, London, 659p.

Long, G. J. and Grandjean, F. (1993) *Mössbauer spectroscopy applied to magnetism and materials scince*. Plenum Press, New York, 479p.

Murad, E. and Cashion, J. (2004) *Mössbauer spectroscopy of environmental materials and their utilization*. Kluwer, Boston, 417p.

O'Reilly, W. (1984) *Rock and mineral magnetism*. Chapman and Hall, London, 220p.

Vandenberghe R. E., De Grave E., Landuydt C., Bowen L. H. (1990) Some aspects concerning the characterization of iron oxides and hydroxides in soils and clays. *Hyp Interact.*, **53**, 175-196.

Vandenberghe R. E., Barrero, C. A., da Costa, G. M., Van San, E., De Grave E. (2000) Mössbauer characterization of iron oxides and (oxy)hydroxides: the present state of the art. *Hyp. Interact.*, **126**, 247-259.

Zhou, Y., Jin, X., Mukovskii, Y. M., Shvets, I. V. (2004) Kinetics of low-index surfaces of magnetite. *J. Phys.:Condens. Matter*, **16**, 1-12.

Table 1 – Hyperfine parameters for Hibtac under-grate samples.

Sample	B_{hf} (T)	QS (mm/s)	IS (mm/s)	%	Site	Ratio	Iron phase
	51.6(1)	-0.19(1)	0.37(1)	12			Hematite
H2P1	49.0(2)	-0.01(1)	0.26(1)	36	A	0.69	Magnetite
	45.9(1)	0.01(1)	0.66(1)	52	B		
	51.7(1)	-0.17(3)	0.37(1)	6			Hematite
H2P3	48.9(1)	-0.02(1)	0.27(1)	37	A	0.65	Magnetite
	45.9(1)	0.01(1)	0.66(1)	57	B		
	51.8(1)	-0.20(1)	0.38(2)	10			Hematite
H2P4	49.1(2)	-0.01(1)	0.27(1)	35	A	0.64	Magnetite
	46.0(1)	0.01(1)	0.65(1)	55	B		
	51.9(3)	-0.17(3)	0.39(1)	6			Hematite
H2P5	49.2(2)	-0.01(2)	0.28(1)	36	A	0.62	Magnetite
	45.9(1)	0.01(1)	0.65(1)	58	B		
	51.6(1)	-0.18(1)	0.37(1)	50			Hematite
H2P6	49.0(2)	-0.02(1)	0.28(1)	19	A	0.61	Magnetite
	46.0(1)	0.01(1)	0.67(1)	31	B		
	50.5(1)	-0.03(1)	0.48(1)	4			Maghemite
H2P8	49.0(1)	-0.01(1)	0.26(1)	35	A	0.57	Magnetite
	45.9(1)	0.02(1)	0.66(1)	61	B		

Table 2 – Hyperfine parameters from Ispat-Inland under-grate samples.

Sample	B_{hf} (T)	QS (mm/s)	IS (mm/s)	%	Site	Ratio	Iron phase
I5S1	49.0(1)	-0.02(1)	0.28(1)	40	A	0.67	Magnetite
	45.9(1)	0.01(1)	0.67(1)	60	B		
I6S2	51.9(1)	-0.21(6)	0.38(3)	8			Hematite
	49.0(1)	-0.04(1)	0.27(1)	36	A	0.64	Magnetite
	46.0(1)	0.01(1)	0.68(1)	56	B		
I6S3	51.7(1)	-0.17(1)	0.39(2)	13			Hematite
	49.0(2)	-0.01(1)	0.27(1)	33	A	0.64	Magnetite
	46.0(1)	0.01(1)	0.65(1)	54	B		
I6S4	51.6(3)	-0.12(6)	0.37(3)	9			Hematite
	48.9(1)	-0.02(2)	0.23(1)	34	A	0.60	Magnetite
	46.0(1)	0.03(1)	0.67(1)	57	B		
I6S5	51.4(4)	-0.15(8)	0.35(5)	8			Hematite
	49.1(1)	-0.01(1)	0.26(1)	35	A	0.61	Magnetite
	46.0(1)	0.01(1)	0.65(1)	57	B		
I6S6	51.6(3)	-0.18(2)	0.36(1)	26			Hematite
	49.0(1)	-0.03(2)	0.25(1)	28	A	0.60	Magnetite
	46.0(1)	0.02(1)	0.66(1)	46	B		
I6S7	51.7(1)	-0.13(1)	0.37(1)	37			Hematite
	48.9(1)	-0.04(1)	0.27(1)	27	A	0.75	Magnetite
	46.1(1)	0.02(1)	0.69(1)	36	B		

Table 3 – Hyperfine parameters from Minntac Line 7 under grate samples.

Sample	B_{hf} (T)	QS (mm/s)	IS (mm/s)	%	Site	Ratio	Iron phase
M4S6	51.6(3)	-0.18(3)	0.37(1)	64			Hematite
	48.9(2)	-0.03(2)	0.28(1)	13	A	0.57	Magnetite
	46.1(1)	0.03(1)	0.67(1)	23	B		
M4S4	51.7(1)	-0.18(1)	0.38(2)	9			Hematite
	49.0(2)	-0.00(1)	0.27(1)	35	A	0.63	Magnetite
	46.0(1)	0.01(1)	0.65(1)	56	B		
M4S2	51.9(2)	-0.15(4)	0.39(2)	9			Hematite
	49.0(1)	-0.01(1)	0.26(1)	36	A	0.65	Magnetite
	46.0(1)	0.01(1)	0.66(1)	55	B		
M5S1	49.0(2)	-0.04(1)	0.27(1)	38	A	0.61	Magnetite
	46.0(1)	0.02(1)	0.67(1)	62	B		

Table 4 – Hyperfine parameters from United Taconite under-grate samples.

Sample	B_{hf} (T)	QS (mm/s)	IS (mm/s)	%	Site	Ratio	Iron phase
U5S1	49.0(1)	-0.03(1)	0.26(1)	39	A	0.55	Magnetite
	46.0(1)	0.01(1)	0.66(1)	66	B		
U5S5	51.6(1)	-0.17(3)	0.37(1)	63			Hematite
	48.9(1)	-0.02(1)	0.26(1)	12	A	0.48	Magnetite
	45.8(1)	0.01(1)	0.70(1)	25	B		
U5S7	51.6(1)	-0.18(1)	0.37(2)	65			Hematite
	48.9(1)	-0.01(2)	0.28(1)	13	A	0.59	Magnetite
	45.9(1)	0.01(1)	0.66(1)	22	B		

Table 5 – Hyperfine parameters from scrubber solids.

Sample	B_{HF} (T)	QS (mm/s)	IS (mm/s)	%	Site	Ratio	Iron phase
Hibtac	51.7	-0.18	0.38	72			Hematite
	48.9	-0.05	0.30	10	A	0.56	Magnetite
	46.1	-0.05	0.71	18	B		
Hibtac 2	51.6	-0.19	0.37	73			Hematite
	49.0	-0.07	0.26	10	A	0.59	Magnetite
	45.9	-0.02	0.69	17	B		
Ispat	51.7	-0.18	0.37	79			Hematite
	48.5	0.09	0.31	9	A	0.75	Magnetite
	45.8	0.03	0.68	12	B		
Minntac	51.7	-0.18	0.36	16			Hematite
	49.2	-0.05	0.26	35	A	0.71	Magnetite
	46.0	-0.03	0.66	49	B		
United	51.7	-0.18	0.36	48			Hematite
	49.2	-0.07	0.27	22	A	0.73	Magnetite
	45.9	0.02	0.67	30	B		

Table 6 – Hyperfine parameters for products from heated greenball experiments.

Sample	B_{HF} (T)	QS (mm/s)	IS (mm/s)	%	Site	Ratio	Iron phase
GB	49.5	-0.02	0.29	42	A	0.72	Magnetite
	45.9	0.00	0.64	58	B		
GB400A	52.0	-0.14	0.39	11			Hematite
	49.5	-0.04	0.28	44	A	0.98	Magnetite
	45.9	0.00	0.65	45	B		
GB500A	51.8	-0.14	0.37	23			Hematite
	49.1	-0.06	0.26	43	A	1.26	Magnetite
	46.3	0.05	0.71	34	B		
GB500N	50.5	0.16	0.43	11			Hematite (?)
	49.2	-0.07	0.25	33	A	0.59	Magnetite
	45.9	0.04	0.65	56	B		
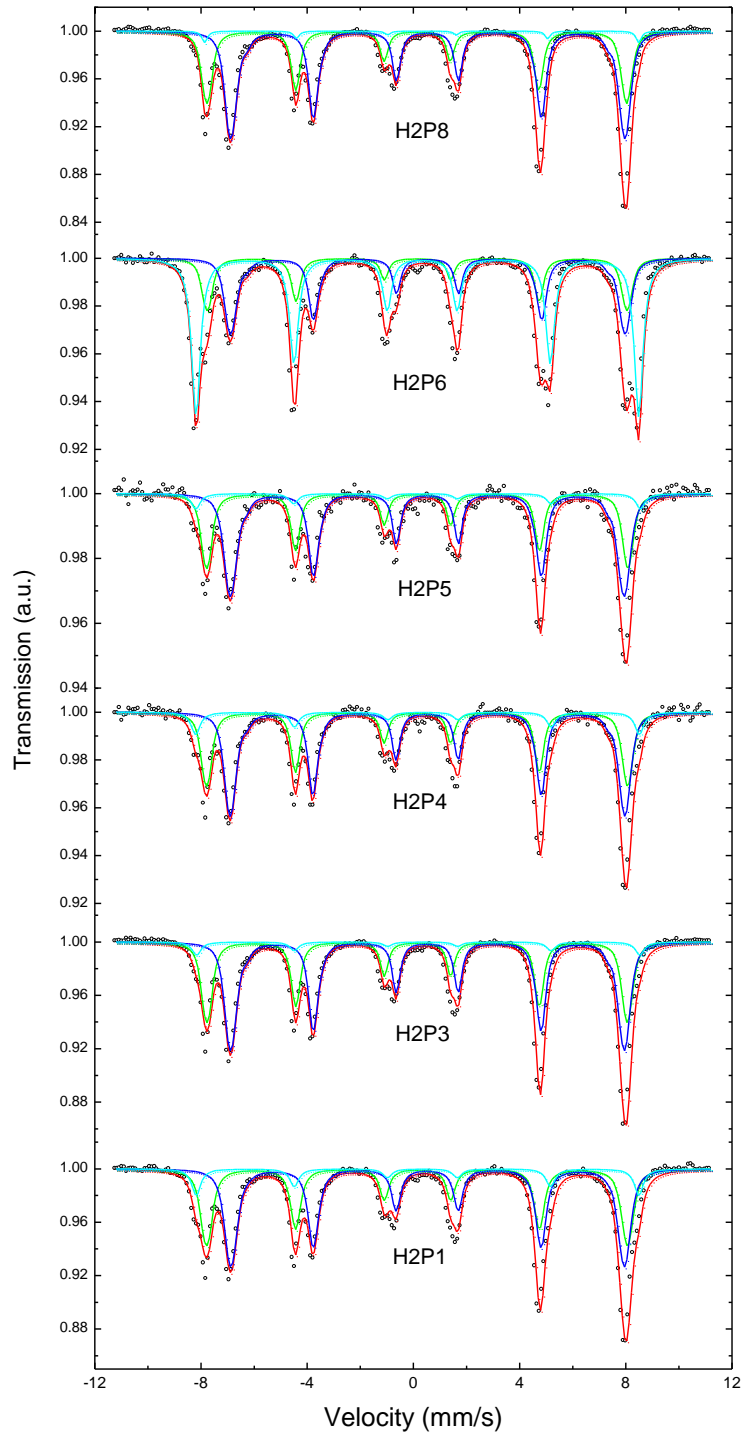
Figure 1 - Mössbauer spectra from Hibtac under-grate samples.
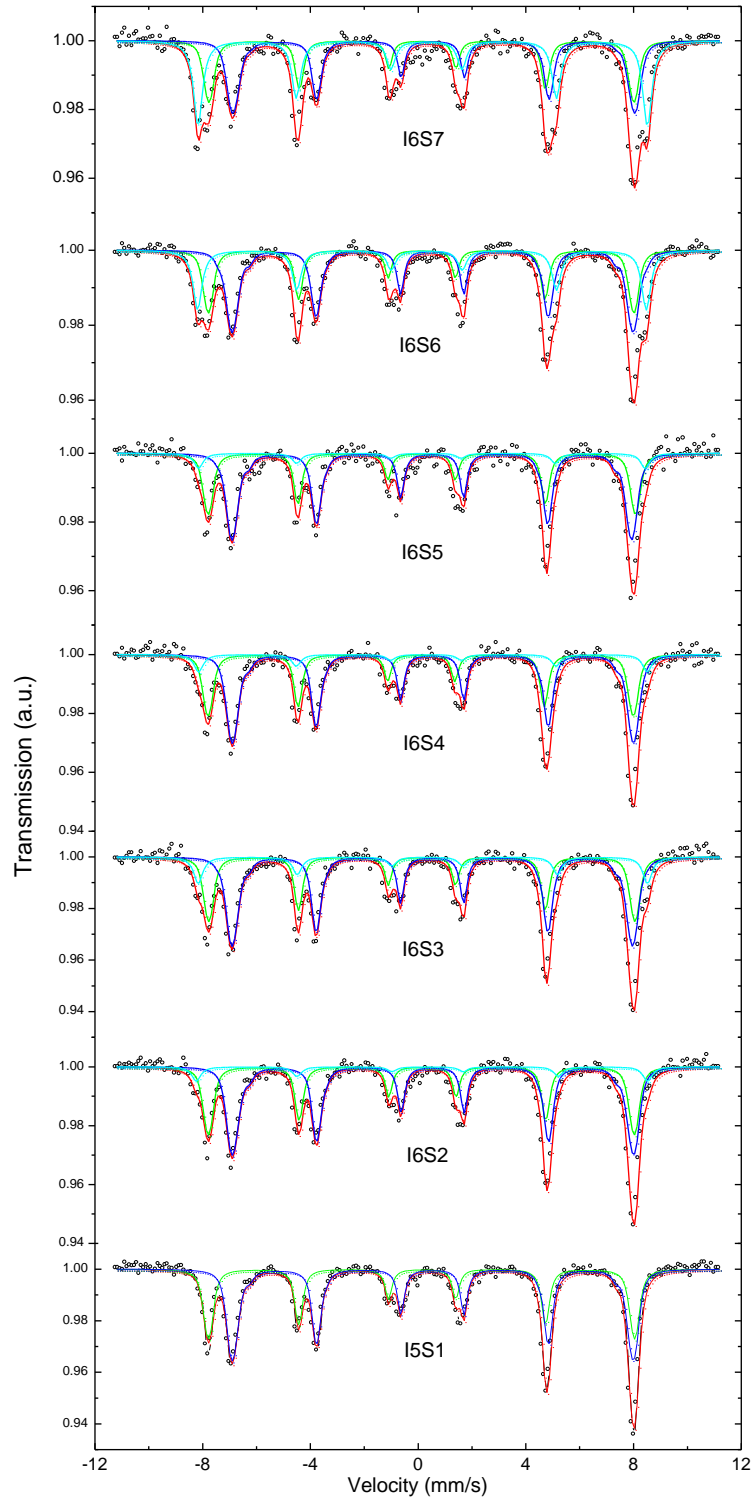
Figure 2 - Mössbauer spectra from Ispat Inland under-grate samples.
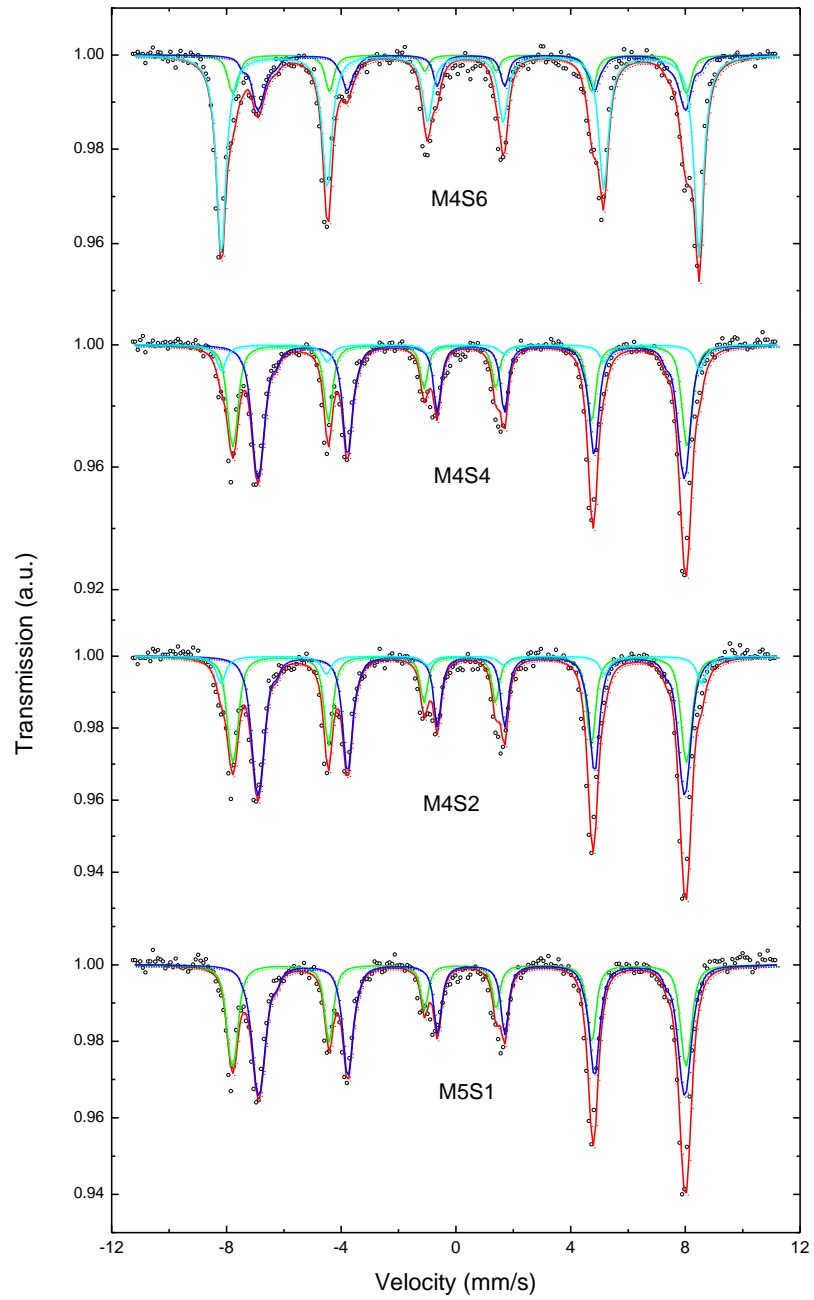
Figure 3 - Mössbauer spectra from Minntac Grate samples.
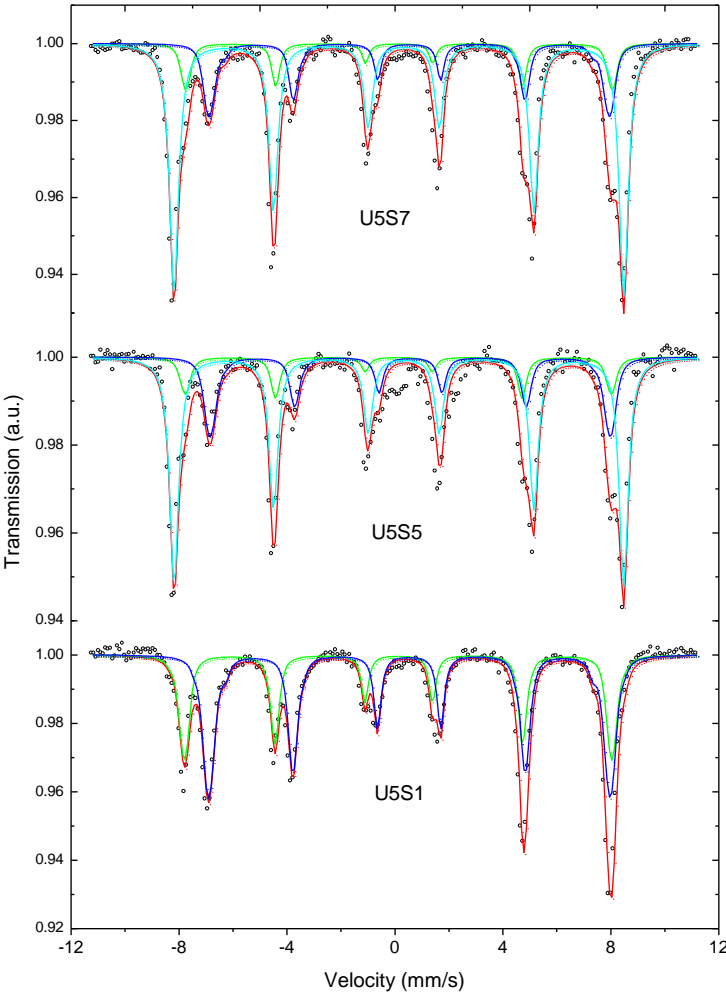
Figure 4 - Mössbauer spectra from United Taconite Grate samples.
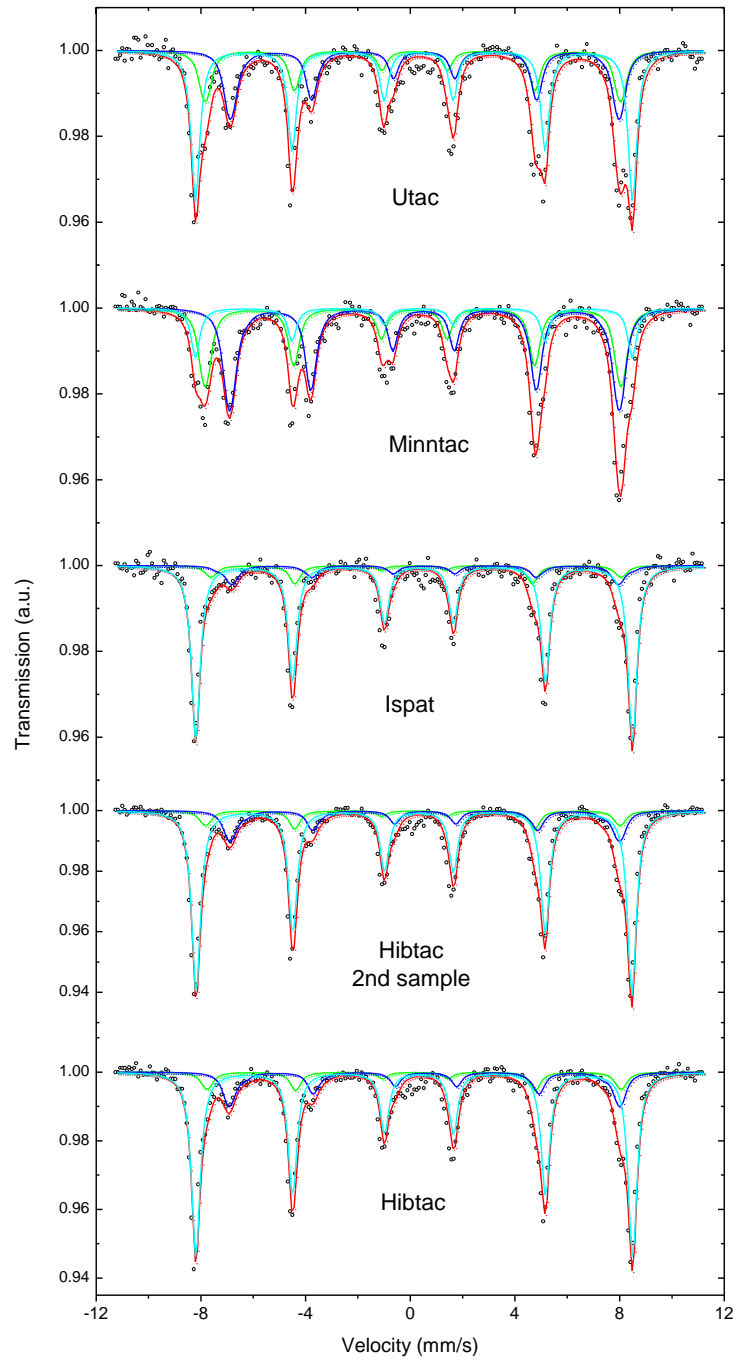
Figure 5 - Mössbauer spectra from scrubber solids.
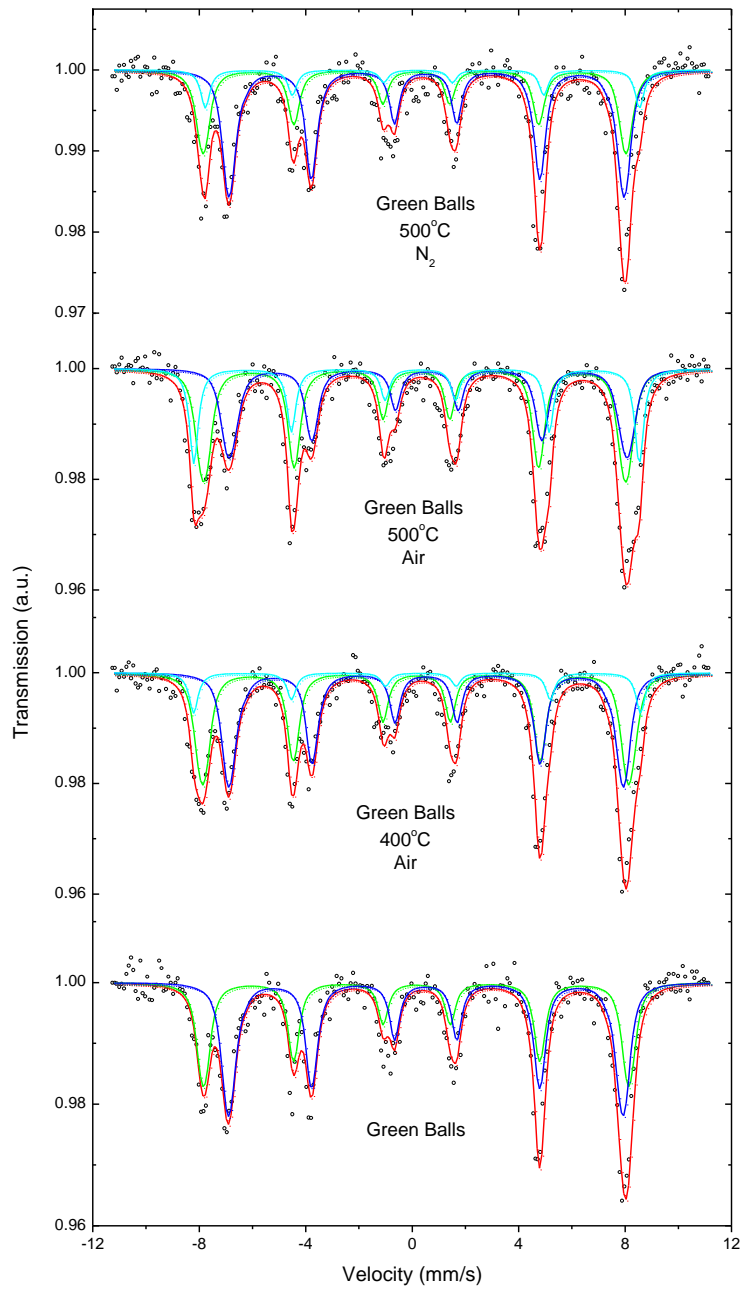
Figure 6 - Mössbauer spectra from heated Minntac greenball samples.

9.5. Raw Mercury Data

Hibtac

	DNR 2003 Study	Hg(D)	Hg(P)	TSS	Hg(T)
2/20/2003		ng/l	ng/g	wt%	ng/l
Hg6	Scrubber Water, filtered after 5 days	13.5	5027.4	0.01226	629.9
Hg8	Scrubber Water, filtered immediately	255.5	1405.5	0.007	353.9
Hg1	Multiclone Dust in proc. water, filtered 5 days	5.2	175.2		
Hg3	Multiclone Dust in proc. water, filtered 5 days	11.7	129.9		
Average		**255.5**	**1405.5**	**0.00963**	**492**
5/8/2003					
2-1	Scrubber Water, filtered immediately	337.3	420.2	0.035	484.4
2-3	Scrubber Water, filtered immediately	340.8	791	0.035	617.7
2-5	Scrubber Water, filtered after 6 days	13.6	1519	0.0328	511.8
2-6	Scrubber Water, filtered after 6 days	13	1539.3	0.0325	513.3
Average		**339.05**	**605.6**	**0.033433**	**532**
	Round 1				
9/11/2003					
H1W1	Scrubber Water, filtered immediately	257.2	597.1	0.038	484.1
H1W2	Scrubber Water, filtered immediately	204.5	610.2	0.038	436.4
Average		**230.85**	**603.65**	**0.038**	**460**
1/27/2004	**Round 2**				
H2W1	Scrubber Water, filtered immediately	301.5	1549	0.0178	577.2
H2W2	Scrubber Water, filtered immediately	281.6	1419	0.0178	534.2
Average		**291.55**	**1484**	**0.0178**	**556**
H2Blank1	Filtered DI Water				
H2Blank2	Unfiltered DI Water				
H2P1	Grate Dust (Windbox 18)		21.8		
H2P2	Grate Dust (Windbox 16)		127.2		
H2P3	Grate Dust (Windbox 14)		463.6		
H2P4	Grate Dust (Windbox 12)		93.5		
H2P5	Grate Dust (Windbox 8)		19.3		
H2P6	Grate Dust (Scraped between WB 6 and 7)		31.8		
H2P7	Grate Dust (Scraped between WB 2 and 3)		17.9		
H2P8	Greenball (dried)		10.9		
5/12/2004	**Round 3**				
H3W1	Scrubber Water, filtered immediately	63	2363	0.013	370.2
H3W2	Scrubber Water, filtered immediately	410.4	1715	0.013	633.4
Average		**236.7**	**2039**	**0.013**	**502**
H3W3	Rougher feed, Decanted, Filtered	4.7			
H3W4	Rougher feed, Decanted, Filtered	4.3			

H3Blank1	Filtered DI Water	1.7			
H3Blank2	Unfiltered DI Water	1.1			
H3S1	Greenball		16.5		

7/27/2004 Round 4

H4W1	Scrubber Water, filtered immediately	282.5	2710.9	0.0139	659.3
H4W2	Scrubber Water, filtered immediately	305.4	2914.6	0.0136	701.8
H4W3	Scrubber Water, Filtered at 5 Min	269.5	3096.4	0.0136	690.6
H4W4	Scrubber Water, Filtered at 10 Min	422.3	2712.3	0.0136	791.2
H4W5	Scrubber Water, Filtered at 15 Min	215.1	3300.1	0.0136	663.9
H4W6	Scrubber Water, Filtered at 30 Min	169.8	3581.1	0.0136	656.8
H4W7	Scrubber Water, Filtered at 60 Min	129.9	3859.5	0.0136	654.8
Average		**293.95**	**2812.75**	**0.013643**	**688**
H4Blank1	Filtered DI Water	3.2			
H4Blank2	Unfiltered DI Water	3.4			
H4S1	Greenball		20.6		

Round 5
Lines shut down when we arrived.

2/15/2005 Round 6

H6W1	Scrubber Water, filtered immediately	607.5	3147.1	0.024	1362.8
H6W2	Scrubber Water, filtered immediately	833.7	2601.3	0.024	1458.0
Average		**720.6**	**2874.2**	**0.024**	**1410**
H6N1	Non Magnetic Fraction, 5 mls tails, 245 mls scrubber water		1912.4		
H6N3	Non Magnetic Fraction, 10 mls tails, 240 mls scrubber water		1012.1		
H6N4	Non Magnetic Fraction, 10 mls tails, 240 mls di-water		57.7		
H6N5	Non Magnetic Fraction Scrubber Water		7387.1		
H6M1	Magnetic Fraction, 5 mls tails, 245 mls sw		784.8		
H6M3	Magnetic Fraction, 10 mls tails, 240 mls sw		539.8		
H6M4	Magnetic Fraction, 10 mls tails, 240 mls di-water		99.8		
H6M5	Magnetic Fraction Scrubber Water Solids		2521.714		
H6Blank1	Filtered DI Water	2.9			
H6Blank2	Unfiltered DI Water	2.3			
H6S1	Greenball		18.6		

5/19/2005 Round 7

H7W1	Scrubber Water, filtered immediately	258.9	6407	0.0073	726.6
H7W2	Scrubber Water, filtered immediately	249.3	9178	0.0057	772.4
H7W3	Scrubber Water, filtered immediately	194.2	9603	0.0052	693.6
Average		**234.1333**	**8396**	**0.006067**	**731**

H7B1	Filtered DI Water	2.5	4.9	
H7B2	Unfiltered DI Water	1.8		
H7S1	Greenball Feed Sample		26.4	

Minntac

Minntac		Hg(D) ng/l	Hg(P) ng/g	TSS wt%	Hg(T) ng/l
	DNR 2003 Study				
2/19/2003					
Hg1	Scrubber Water Line 4 (filtered after 6 days)	26.9	2306.5	0.05179	1221.4
Hg2	Scrubber Water Line 4 (filtered after 6 days)	22.9	1864.2	0.06318	1200.7
Hg3	Scrubber Water Line 4 (filtered immediately)	115.8	1284.8	0.086	1220.7
Hg5	Scr. Water Line 4 (acidified to pH 3, filtered 6 days)	68.3	1970.3	0.05789	1208.9
Hg6	Scr. Water Line 4 (acidified to pH 4.5, filtered 6 days)	22.3	2093.7	0.05201	1111.2
Hg8	Scr. Water Line 4 (NaOH add to pH 9, filtered 6 days)	16.9	2607.7	0.0391	1036.5
Average		**115.8**	**1284.8**	**0.058328**	**1166.6**
5/9/2003					
2-1	scrubber water **line 4** filtered immediately	89.8	153	0.387	681.9
2-3	scrubber water **line 4** filtered immediately	72.6	167.6	0.387	721.2
2-5	scrubber water (filtered after 6 days)	25.7	179.9	0.2423	461.6
2-6	scrubber water (filtered after 6 days)	26.7	173.8	0.2423	447.8
Average		**81.2**	**160.3**	**0.31465**	**578.1**
	Round 1				
9/10/2003					
M1W1	scrubber water **line 4** filtered immediately	264	484.3	0.217	1314.9
M1W2	scrubber water **line 4** filtered immediately	684.5	383.2	0.217	1516.0
20t-1	filtered upon return to lab (approx 3 hr, 20C)	92.8	1620	0.217	3608.2
20t-2	filtered after 22 hours (20 C)	51.7	876.5	0.217	1953.7
40t-1	filtered after 30 min. (40 C)	193.8	758.4	0.217	1839.5
40t-2	filtered after 60 min. (40 C)	305.2	634	0.217	1681.0
60t-1	filtered after 30 min.(60 C)	364.3	659.9	0.217	1796.3
60t-2	filtered after 60 min. (60 C)	164.2	953.1	0.217	2232.4
Average		**474.25**	**433.75**	**0.217**	**1992.8**
1/28/2004	**Round 2**				
M2W1	scrubber water **line 4** filtered immediately	159	1264.4	0.145	1992.4
M2W2	scrubber water **line 4** filtered immediately	168	1850.3	0.145	2850.9
Average		**163.5**	**1557.35**	**0.145**	**2421.658**
M2W7	scrubber water **line 7**, filtered immediately	210.6	2647.1	0.0413	1303.9
M2W8	scrubber water **line 7**, filtered immediately	235.6	2331.3	0.0413	1198.4
Average		**223.1**	**2489.2**	**0.0413**	**1251.14**

M2W3	scrubber thickener underflow, filtered immediately	16.3	37.2	35.73	13307.9
M2W5	overflow from scrubber thickener	109.3	325.5	0.0076	134.0
M2W6	overflow from thickener (not filtered)				139.6
5/11/2004	**Round 3**				
M3W1	scrubber water line 7, filtered immediately	291.3	2182.2	0.052	1426.0
M3W2	scrubber water line 7, filtered immediately	290	3262.8	0.052	1986.7
Average		**290.65**	**2722.5**	**0.052**	**1706.35**
M3W3	Lines 6 & 7 agglomerator to concentrator, filtered immediately	3.7	55.6	0.12	70.4
M3W4	Lines 6 & 7 agglomerator to concentrator, filtered immediately	5.0	35.1	0.12	47.1
M3B1	filtered DI water	2.3	1.2		
M3B2	unfiltered DI water	1.2			
M3S1	greenball feed sample		8.1		
7/27/2004	**Round 4**				
M4W1	scrubber water line 7, filtered immediately	269.7	3144.9	0.0952	3263.6
M4W2	scrubber water line 7, filtered immediately	340	1982.7	0.0952	2227.5
Average		**304.85**	**2563.8**	**0.0952**	**2745.588**
M4B1	filtered DI water	3.7	0.1		
M4B2	unfiltered DI water	2.4			
M4S1	greenball feed sample		11.6		
M4S2	DD1 dust in water, filtered, dried		91.3		
M4S3	DD2 dust in water, filtered, dried		56.6		
M4S4	DD2 dust in water, filtered, dried		66.1		
M4S5	windbox 1 in preheat zone (dry dust)		14.9		
M4S6	windbox 2 in preheat zone (dry dust)		2.8		
M4S7	windbox 3 in preheat zone, (dry dust)		0.7		
12/1/2004	**Round 5**				
M5W1	scrubber water line 7, filtered immediately	204.8	2942	0.075	2411.3
M5W2	scrubber water line 7, filtered immediately	263.8	2717.5	0.075	2301.9
Average		**234.3**	**2829.75**	**0.075**	**2356.613**
M5B1	filtered DI water	2.9	2.6		
M5B2	unfiltered DI water	3.2			
M5S1	greenball feed sample		8.5		
M5M1	Magnetic fraction, tails plus scrubber water (20 hrs)		22		
M5M2	Magnetic fraction, tails plus scrubber water		24.8		
M5M3	Magnetic fraction, tails plus scrubber water		26.3		
M5M4	Magnetic fraction, tails plus DI water		24.2		
M5M5	Magnetic fraction, scrubber water		304.7		

M5N1	Non-Magnetic fraction, tails plus scrubber water	44.3			
M5N2	Non-Magnetic fraction, tails plus scrubber water	36.1			
M5N3	Non-Magnetic fraction, tails plus scrubber water	28			
M5N4	Non-Magnetic fraction, tails plus DI water	29.5			
M5N5	Non-Magnetic fraction, scrubber water	26072.8			

2/16/2005 Round 6

M6W1	line 7 filtered scrubber water	198.7	3171.2	0.058	2038.0
M6W2	line 7 filtered scrubber water	463.7	2538.1	0.058	1935.8
Average		**331.2**	**2854.65**	**0.058**	**1986.897**

M6B1	filtered DI water	6.5	2.3		
M6B2	unfiltered DI water	6.6			
M6S1	greenball feed sample		12		
M6N1	non-magnetic fraction of scrubber water (after 1 day)		9190.8		
M6M1	magnetic fraction of scrubber water (after 1 day)		221.6		

5/20/2005 Round 7

M7W1	scrubber water line 7, filtered immediately	194.5	1424.5	0.097	1576.3
M7W2	scrubber water line 7, filtered immediately	272.9	1426.6	0.098	1671.0
M7W3	scrubber water line 7, filtered immediately	301.5	1228.3	0.105	1591.2
Average		**256.3**	**1359.8**	**0.1**	**1612.816**

M7B1	Filtered DI water	3.9	9.9		
M7B2	Unfiltered DI water	2.3			
M7S1	Greenball Feed Sample		16.1		

U-Tac

United Taconite		Hg(D) ng/l	Hg(P) ng/g	TSS wt%	Hg(T) ng/l
	DNR 2003 Study				
2/18/2003	(EVTAC)				
Hg1	Scrubber thickener underflow (filtered after 7 days)	108.2	496.6	0.5405	2792.3
Hg2	Scrubber thickener underflow (filtered after 7 days)	76.4	436.6	0.8676	3864.3
Hg3	Scrubber thickener underflow (filtered immediately)	64.2	978.7	1.34	13178.8
Average		**64.2**	**978.7**	**0.916033**	**6611.8**

5/8/2003

Mine shutdown

Round 1

9/11/2003

Mine shutdown

1/27/2004 Round 2

U2W2	Scrubber thickener underflow (filtered immediately)	79.3	644.7	0.903	5900.9

U2W3#	Scrubber thickener underflow (filtered immediately)	815.8#	692.9	0.903	
U2W4	Scrubber thickener underflow (filtered immediately)	79.3	656.1	0.903	6003.9
U2W5	Scrubber thickener underflow (filtered immediately)	119.2	796.1	0.903	7308.0
Average		**92.6**	**698.9667**	**0.903**	**6404.269**
5/11/2004	**Round 3**				
U3W1	Scrubber thickener underflow (filtered immediately)	242.9	541.4	1.27	7118.7
U3W2	Scrubber thickener underflow (filtered immediately)	85.8	647.5	1.27	8309.1
Average		**164.35**	**594.45**	**1.27**	**7713.865**
U3W3	agglomerator to concentrator	11.1	115.1	0.497	583.1
U3W4	agglomerator to concentrator	12.9	117	0.497	594.4
U3B1	filtered DI water	1.5			
U3B2	unfiltered DI water	1.3			
U3S1	Greenball feed		13.2		
7/28/2004	**Round 4**				
U4W1	Scrubber thickener underflow (filtered immediately)	135.9	357.5	2.26	8215.4
U4W2	Scrubber thickener underflow (filtered immediately)	88.5	561	2.26	12767.1
Average		**112.2**	**459.25**	**2.26**	**10491.25**
U4B1	filtered DI water	2.3			
U4B2	unfiltered DI water	1.1			
U4M1	Magnetic fraction, tails and s.w. mixture, approx 20 hrs		69		
U4M2	Magnetic fraction, tails and s.w. mixture, approx 20 hrs		58.3		
U4M3	Magnetic fraction, tails and s.w. mixture, approx 20 hrs		64.2		
U4M4	Magnetic fraction, tails(20%) plus DI water, approx 20 hrs		25		
U4M5	Magnetic fraction, scrubber solids, 20 hrs		182.4		
U4N1	Non-Magnetic fraction, tails and sw mixture, 20 hrs		88.3		
U4N2	Non-Magnetic fraction, tails and sw mixture, 20 hrs		74.8		
U4N3	Non-Magnetic fraction, tails and sw mixture, 20 hrs		61.2		
U4N4	Non-Magnetic fraction, tails(20%) plus DI water, 20 hrs		16.7		
U4N5	Non-Magnetic fraction, scrubber solids, 20 hrs		1237.4		
U4S1	Greenball Feed Sample		12.4		
11/29/2004	**Round 5**				
U5W1	Scrubber thickener underflow (filtered immediately)	38.1	264.9	2.41	6422.2
U5W2	Scrubber thickener underflow (filtered immediately)	26.6	379	2.41	9160.5
Average		**32.35**	**321.95**	**2.41**	**7791.345**
U5B2	unfiltered DI water	4.6			
U5S1	Greenball Feed Sample		13.8		
U5S2	Launderers in down draft zone, east side line 2		23.9		
U5S3	Launderers in down draft zone, east side line 2		24.2		
U5S4	Launderers in down draft zone, east side line 2		20.5		
U5S5	Launderers in down draft zone, east side line 2		23.5		

U5S6	multi-tube samples, preheat zone		1.7		
U5S7	multi-tube samples, preheat zone		1.6		
U5S8	multi-tube samples, preheat zone		1.6		
U5S9	multi-tube samples, preheat zone		2.4		

2/14/2005 Round 6

U6W1	Scrubber thickener underflow (filtered immediately)	1423.8	861.6	2.18	20206.7
U6W2	Scrubber thickener underflow (filtered immediately)	1456.4	834.1	2.18	19639.8
Average		**1440.1**	**847.85**	**2.18**	**19923.23**
U6B1	filtered DI water	2.9			
U6B2	unfiltered DI water	1.2			
U6S1	Greenball Feed Sample		24.3		
U6N1	Non-Magnetic Fraction (Scrubber Water, 3 days)		1312.4		
U6M1	Magnetic Fraction (Scrubber Water, 3 days)		311.4		

5/19/2005 Round 7

U7W1	Scrubber thickener underflow (filtered immediately)	237	944.4	1.26	12136.4
U7W2#	Scrubber thickener underflow (filtered immediately)	3474#	422.7#	0.86	
U7W3	Scrubber thickener underflow (filtered immediately)	82	1038.3	1.09	11399.5
U7W4	Scrubber thickener underflow (filtered immediately)	54.1	1019.4	1.63	16670.3
Average		**124.3667**	**1000.7**	**1.21**	**13402.08**
U7B1	Filtered DI water	3.1	7.3		
U7B2	Unfiltered DI water	3			
U7S1	Greenball Feed Sample		19.5		

Ispat

		Hg(D) ng/l	Hg(P) ng/g	TSS wt%	Hg(T) ng/l
	ISPAT				
	DNR 2003 Study				
2/20/2003					
Hg1	Scrubber water, filtered at lab	35.9	1105.3	0.328	3661.3
Hg2	Scrubber water, filtered at lab	33.7	1012.6	0.328	3355.0
Hg3	Scrubber water, filtered immediately	1215.5	616.8	0.328	3238.6
Average		**1215.5**	**616.8**	**0.328**	**3418.3**
5/8/2003					
2-1	Scrubber water, filtered immediately	849.8	4378.8	0.142	7067.7
2-3	Scrubber water, filtered immediately	853.2	1560.2	0.142	3068.7
2-5	Scrubber water, filtered at lab	585.2	3382.9	0.142	5388.9
2-6	Scrubber water, filtered at lab	529.1	3550.1	0.142	5570.2
Average		**851.5**	**2969.5**	**0.142**	**5273.9**
	Round 1				
9/11/2003					
I1W2	Scrubber water, filtered immediately	1174.3	2224.35	0.175	5066.9
I1W2-A	Half of filter for I1W2		2169.5		
I1W2-B	Other half of filter for I1W2		2279.2		

I1W3	Scrubber water, filtered immediately	1019.7	1890.7	0.175	4328.4
I1W3-A	Half of filter for I1W3		1778.9		
I1W3-B	Other half of filter for I1W3		2002.5		
I1W4	Scrubber water, filtered immediately	902.6	2168	0.175	4696.6
I1W4-A	Half of filter for I1W4		2232.8		
I1W4-B	Other half of filter for I1W4		2103.2		
Average		**1032.2**	**2094.35**	**0.175**	**4697.313**
1/27/2004	**Round 2**				
I2W3	Scrubber water, filtered immediately	367.3	2300.6	0.137	3519.1
I2W4	Scrubber water, filtered immediately	1681.9	825.5	0.137	2812.8
Average		**1024.6**	**1563.05**	**0.137**	**3165.979**
5/12/2004	**Round 3**				
I3W1	Scrubber water, filtered immediately	3536.2	678.1	0.095	4180.4
I3W2	Scrubber water, filtered immediately	3087.5	202.6	0.095	3280.0
Average		**3311.85**	**440.35**	**0.095**	**3730.183**
I3W3	concentrate filtrate water (I3F3)	7.0	54.4		
I3W4	concentrate filtrate water (I3F4)	4.8	30.3		
I3B1	filtered DI water (I3F5)	2.0	0.9		
I3B2	unfiltered DI water	1.4			
I3S1	Greenball		8.9		
7/27/2004	**Round 4**				
	No sample				
11/30/2004	**Round 5**				
I5W1	Scrubber water, filtered immediately	375	1632.6	0.118	2301.5
I5W2	Scrubber water, filtered immediately	400.4	2318.1	0.118	3135.8
Average		**387.7**	**1975.35**	**0.118**	**2718.613**
I5B1	filtered DI water	11.5	1.8		
I5B2	unfiltered DI water	2.8			
I5S1	greenball feed sample		7.2		
I5M1	Magnetic fraction, 137 mls tails to 942 mls sw		47.4		
I5M2	Magnetic fraction, 106 mls tails to 919 mls sw		56.2		
I5M3	Magnetic fraction, 173 mls tails to 970 mls sw		32.4		
I5M4	Magnetic fraction, 202 mls tails to 914 mls sw		23.2		
I5M5	Magnetic fraction, scrubber water only		255.7		
I5N1	Non-Magnetic fraction, 137 mls tails to 942 mls sw		25.5		
I5N2	Non-Magnetic fraction, 106 mls tails to 919 mls sw		38.2		
I5N3	Non-Magnetic fraction, 173 mls tails to 970 mls sw		33.6		
I5N4	Non-Magnetic fraction, 202 mls tails to 914 mls sw		12.3		
I5N5	Non-Magnetic fraction, scrubber water only		2411		
2/15/2005	**Round 6**				

I6W1	Scrubber water, filtered immediately	248	3860.6	0.17	6811.0
I6W2	Scrubber water, filtered immediately	359.4	4202.6	0.17	7503.8
Average		**303.7**	**4031.6**	**0.17**	**7157.42**
I6B1	filtered DI water	4.1	2.3		
I6B2	unfiltered DI water	2.8			
I6N1	Non-Magnetic fraction, scrubber water only		2766.6		
I6M1	Magnetic fraction, scrubber water only		102.2		
I6S1	greenball feed sample		9.9		
I6S2	under-grate sample		7.3		
I6S3	under-grate sample		10.5		
I6S4	under-grate sample		58.1		
I6S5	under-grate sample		57.6		
I6S6	under-grate sample		25.8		
I6S7	under-grate sample		5		
5/19/2005	**Round 7**				
I7W1	Scrubber water, filtered immediately	410.3	2551	0.112	3267.4
I7W2	Scrubber water, filtered immediately	462	2800.1	0.131	4130.1
I7W3	Scrubber water, filtered immediately	467.8	2747	0.114	3599.4
Average		**464.9**	**2773.55**	**0.1225**	**3864.756**
I7B1	filtered DI water	10.1	7.5		
I7B2	unfiltered DI water	10.8			
	Greenball Feed Sample		7.1		